The Raman LIDAR for the pre-production phase of CTA.

Marco Iarlori – marco.iarlori@aquila.infn.it
CETEMPS/DSFC University of L'Aquila – Italy
with
Ermanno Pietropaolo, Vincenzo Rizi, Valerio Silvestri, Alberto Cirella, Carla Aramo, Laura Valore, Marco Marengo and Giovanni Dughera for CTA Collaboration.

INFN Istituto Nazionale di Fisica Nucleare
Sezione di Torino
Sezione di Napoli
Gruppo Collegato GSSI L'Aquila

CETEMPS

DSFC

Dipartimento di Fisica
Ettore Pancini

AtmoHEAD 2018 – Capri (Italy), 24-26 September 2018

How could a Raman lidar be useful for CTA?

aerosol optical depth -> light transmission

aerosol backscatter -> light scattering

water vapour -> air refractive index

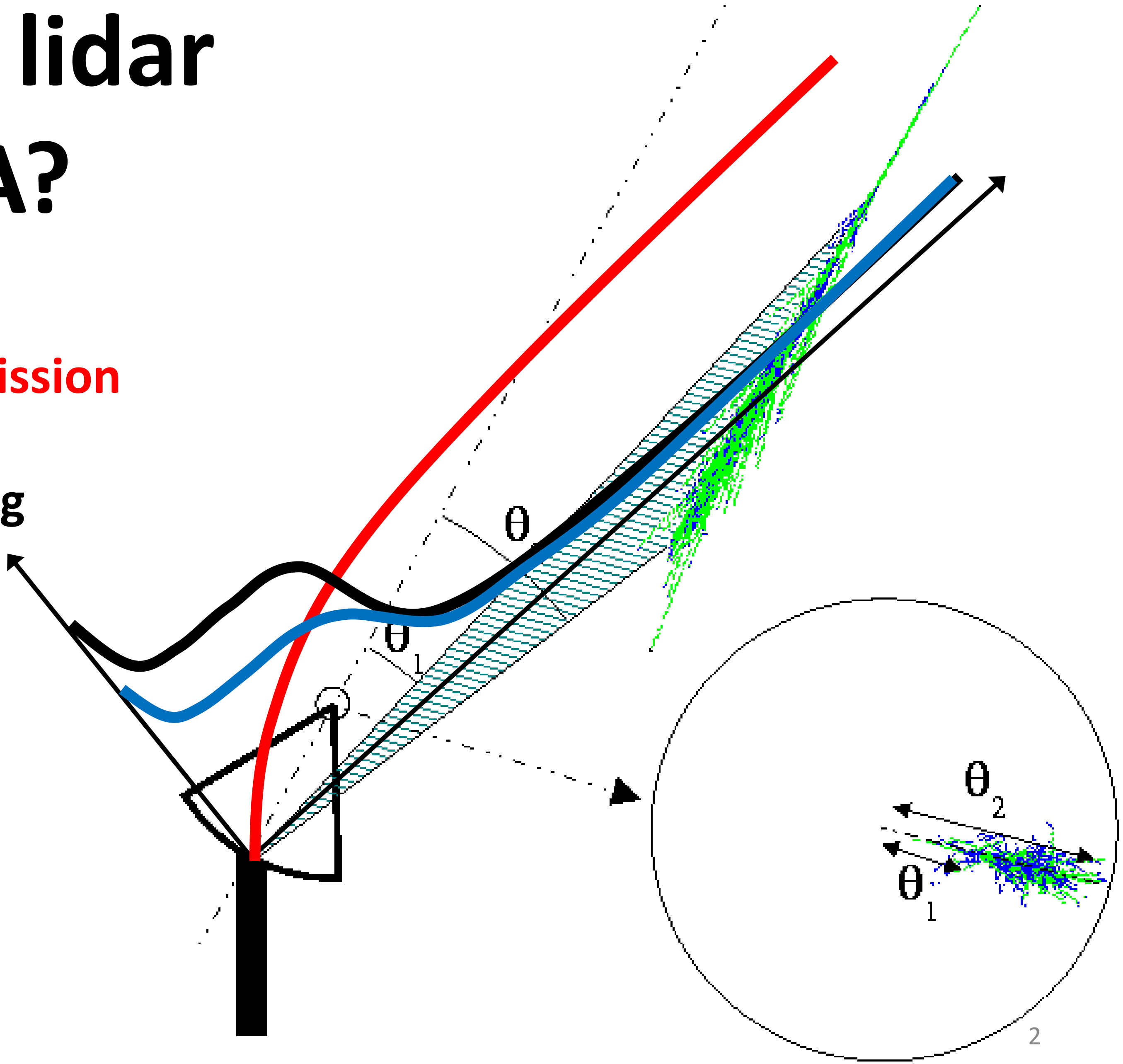

CTA - STATUS ARCADE Raman lidar

The Raman lidar (ARCADE) has undergone several performance tests (hardware/software quality insurance) in the laboratory of the CETEMPS/DSFC/UNIVAQ and INFN at L’Aquila.

ARCADE in lab

ARCADE in lab detectors and telescope

ARCADE in lab laser optical bench

TELESCOPE overall

side view

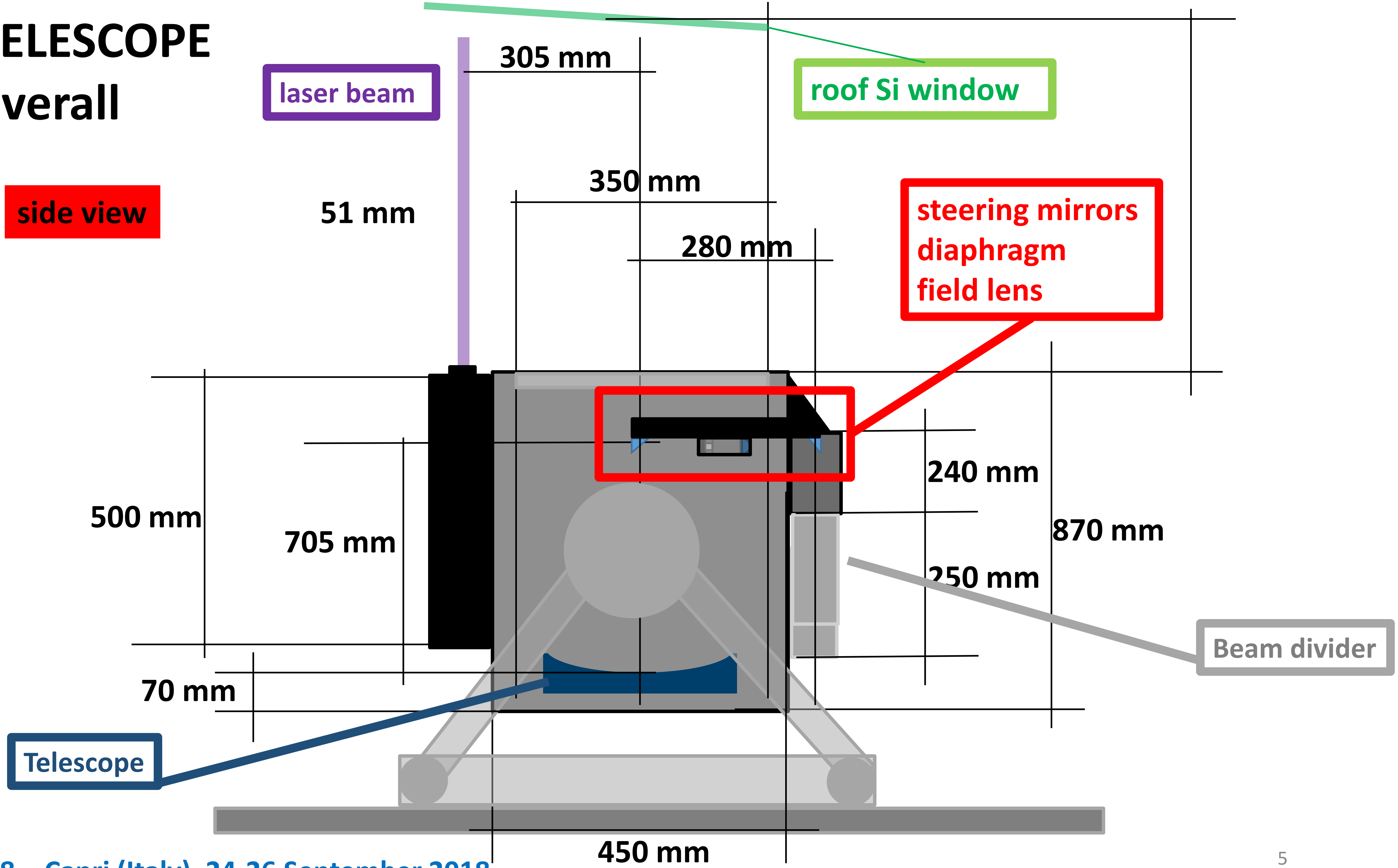

• The Transmitter section

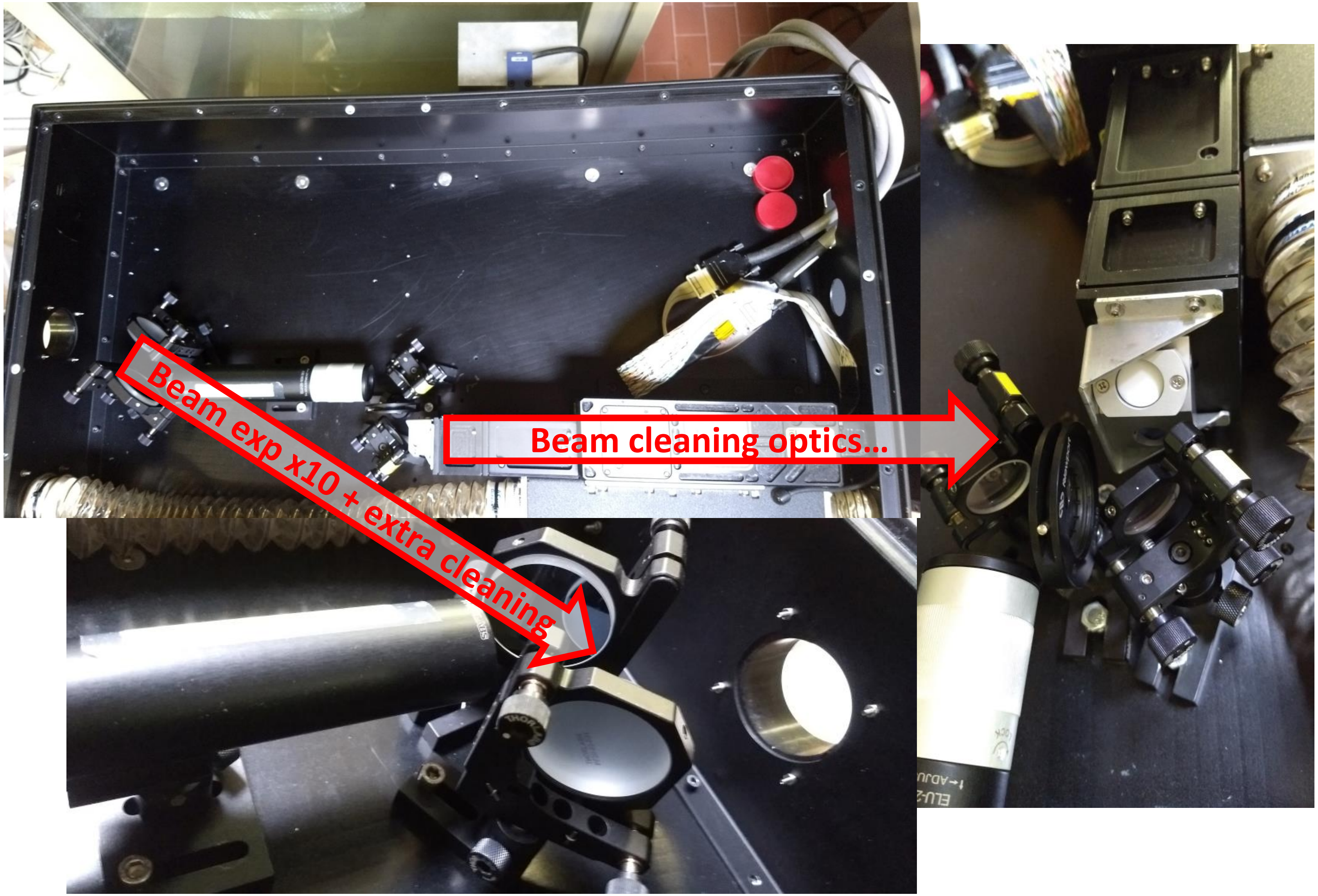

Beam exp x10 + extra cleaning

Beam cleaning optics…

LASER BENCH LAYOUT

ZEMAX© simulation

LASER beam footprint

Overall laser beam half angle divergence: ~ 0.32±0.05 mrad

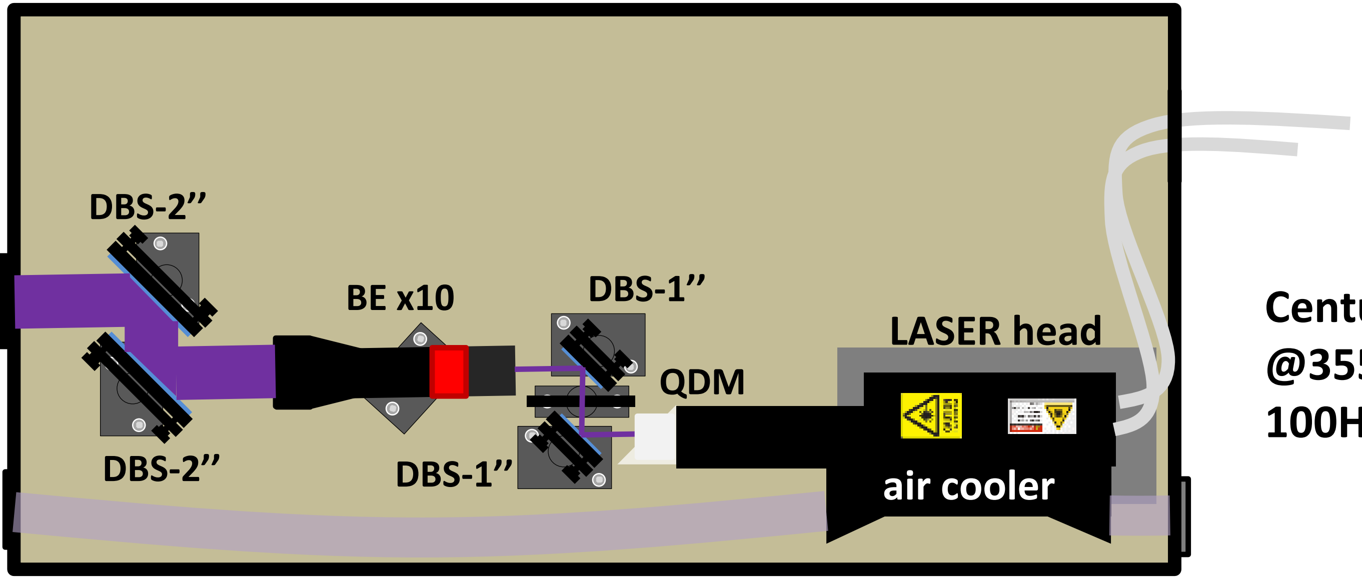

Centurion Laser
@355 nm
100Hz repetition rate

DBS: dichroic beam splitter
BE: beam expander
QDM: quad dichroic module

• The Transmitter section

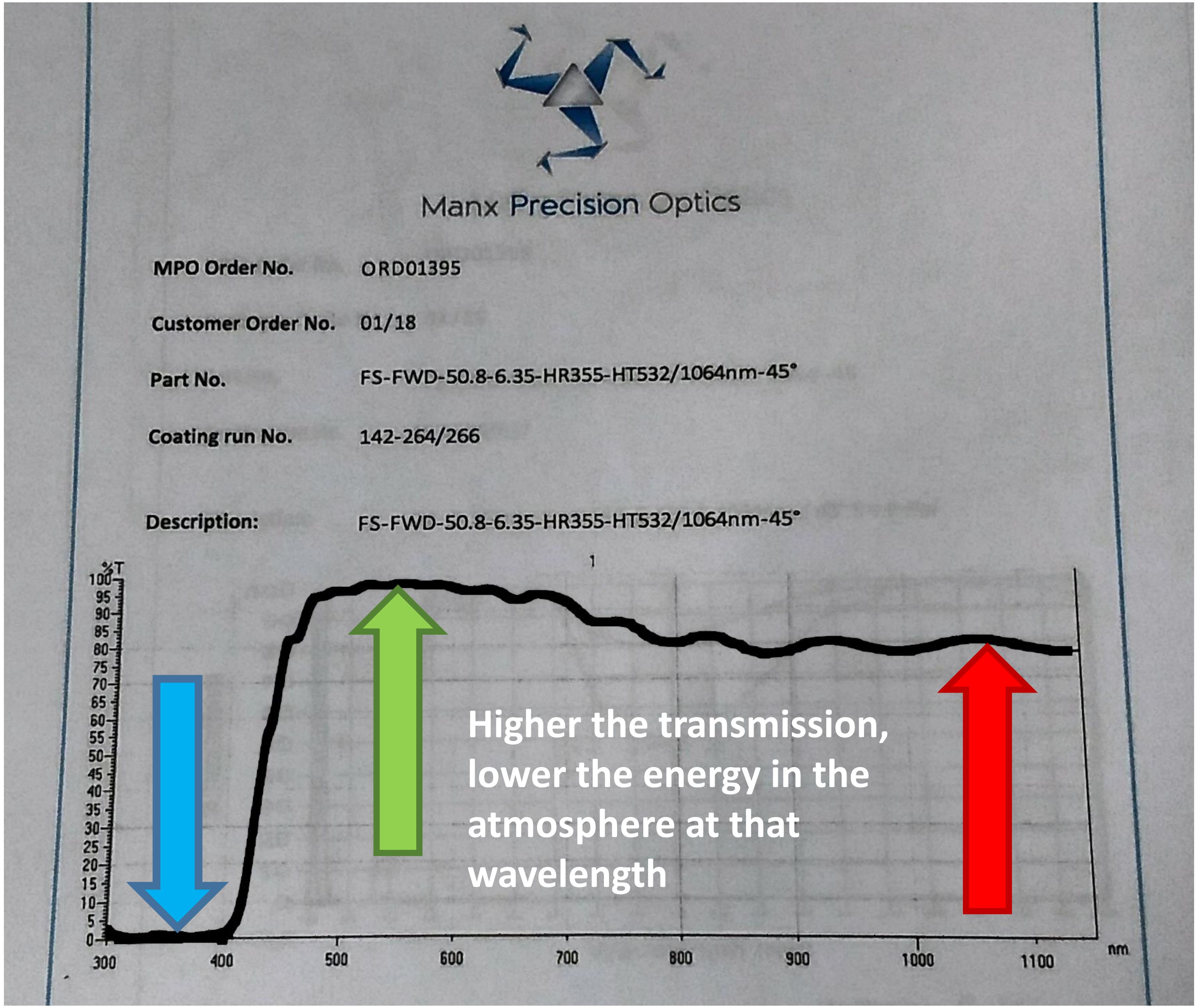

Manx Precision Optics

MPO Order No.	ORD01395
Customer Order No.	01/18
Part No.	FS-FWD-50.8-6.35-HR355-HT532/1064nm-45°
Coating run No.	142-264/266
Description:	FS-FWD-50.8-6.35-HR355-HT532/1064nm-45°

Higher the transmission, lower the energy in the atmosphere at that wavelength

New DBS:

- Beam purity better than 99.9%
- LASER energy per pulse 5.8 ± 0.2 mJ at 354.7 nm

New BEx10:

- Better optical quality

- **The Receiver section**

ZEMAX© simulation

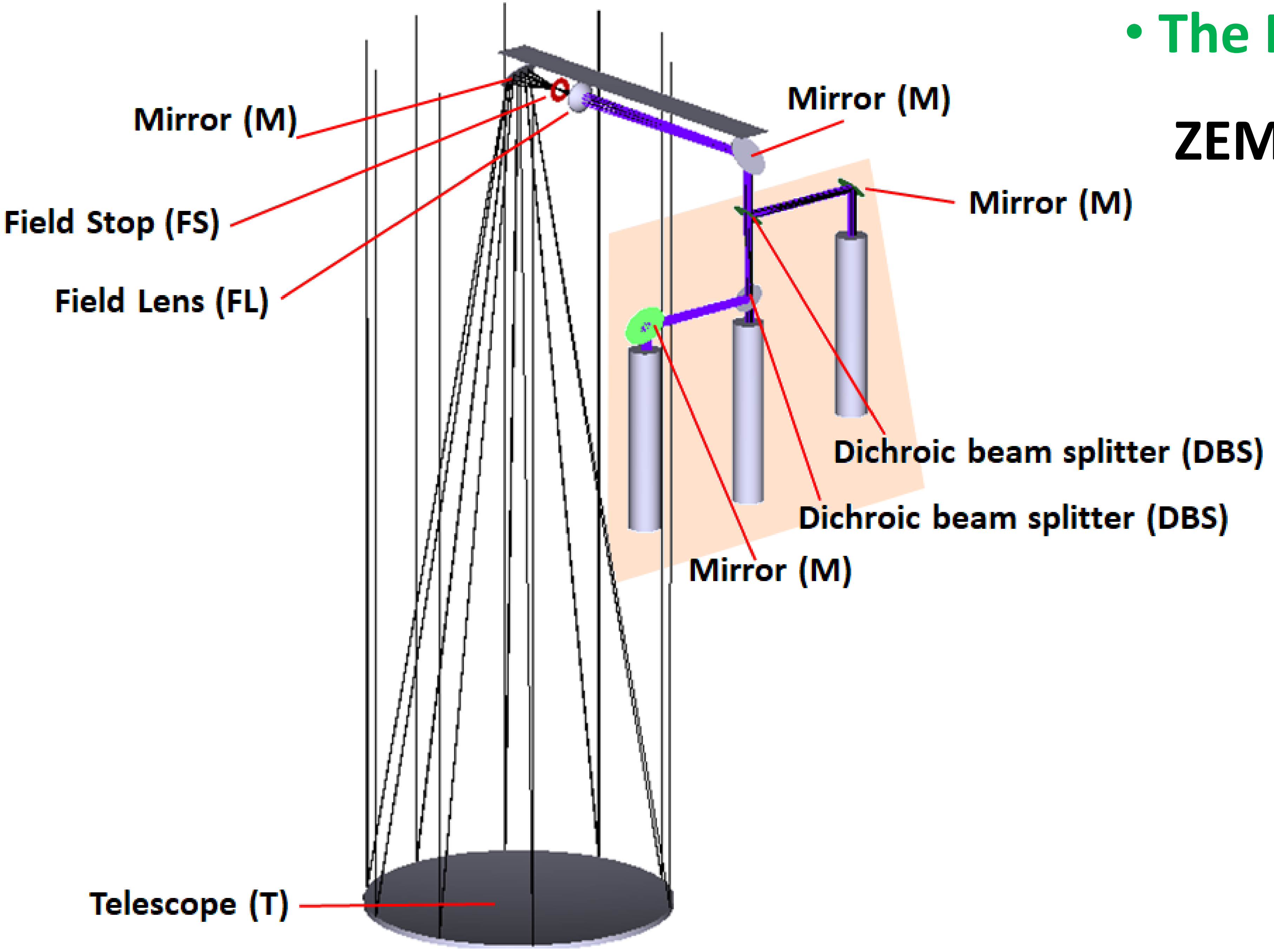

• The Receiver section

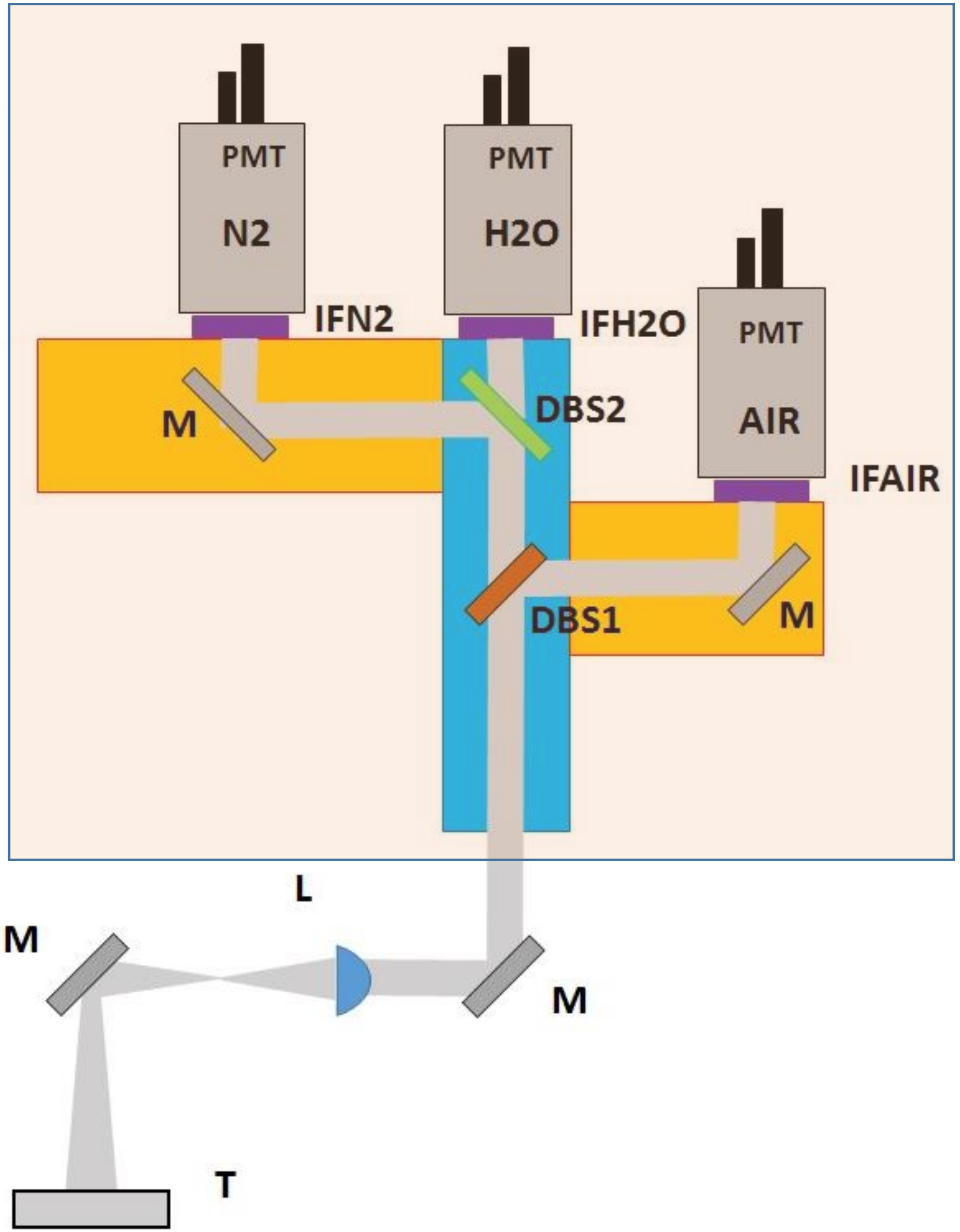

IFN2	interference filter N2	386.7/0.5 nm
IFH2O	interference filter H2O	407.6/1.0 nm
IFAIR	interference filter air	354.7/0.5 nm
DBS1	dichroic beam splitter R 354.7nm T 380-420 nm	
DBS2	dichroic beam splitter R 386.7nm T 400-420 nm	
M	Elliptical Mirror 26.97mm Minor Axis UV Enhanced Aluminum Edmund optics	
L	LA1805-A lens, f = 30 mm	
T	Marcon Telescope, 25cm f/3 Aluminum-Magnesium Fluoride Coating Al + MgF2	

• The Receiver section

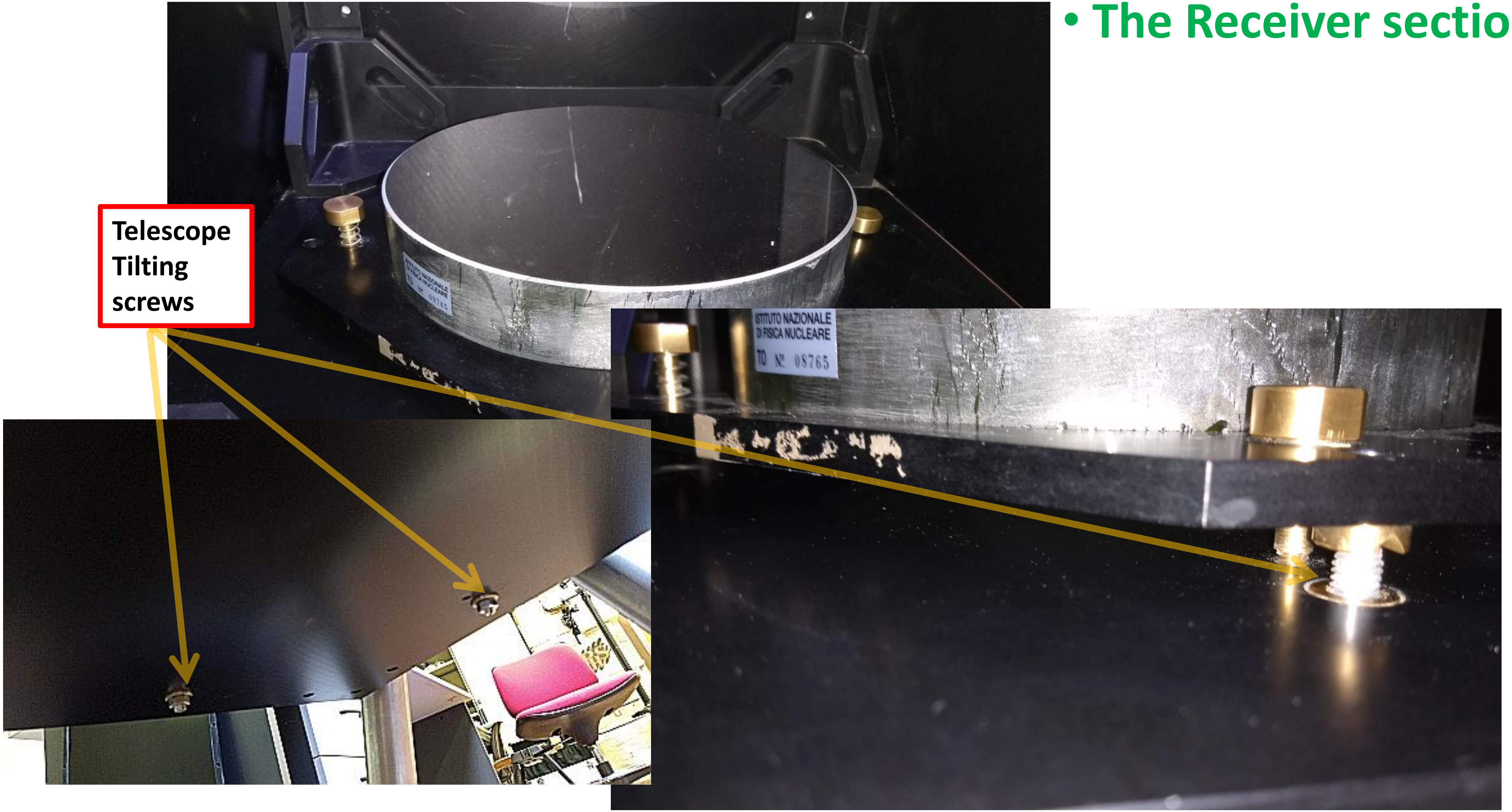

Telescope Tilting screws

• The Receiver section

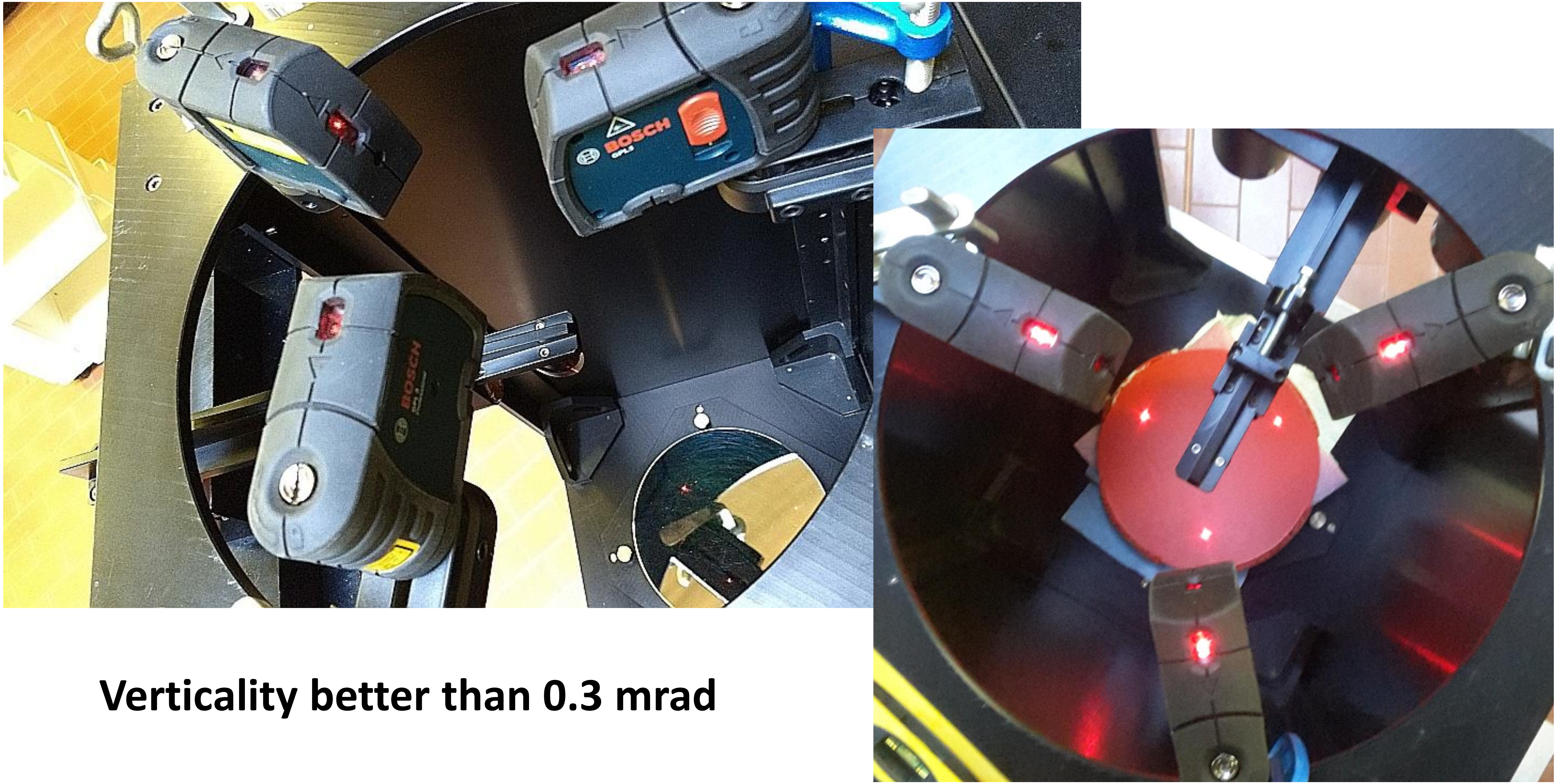

Verticality better than 0.3 mrad

- The Receiver section

steering mirrors
diaphragm
field lens

• The Receiver section

steering mirrors
diaphragm
field lens

- The Receiver section

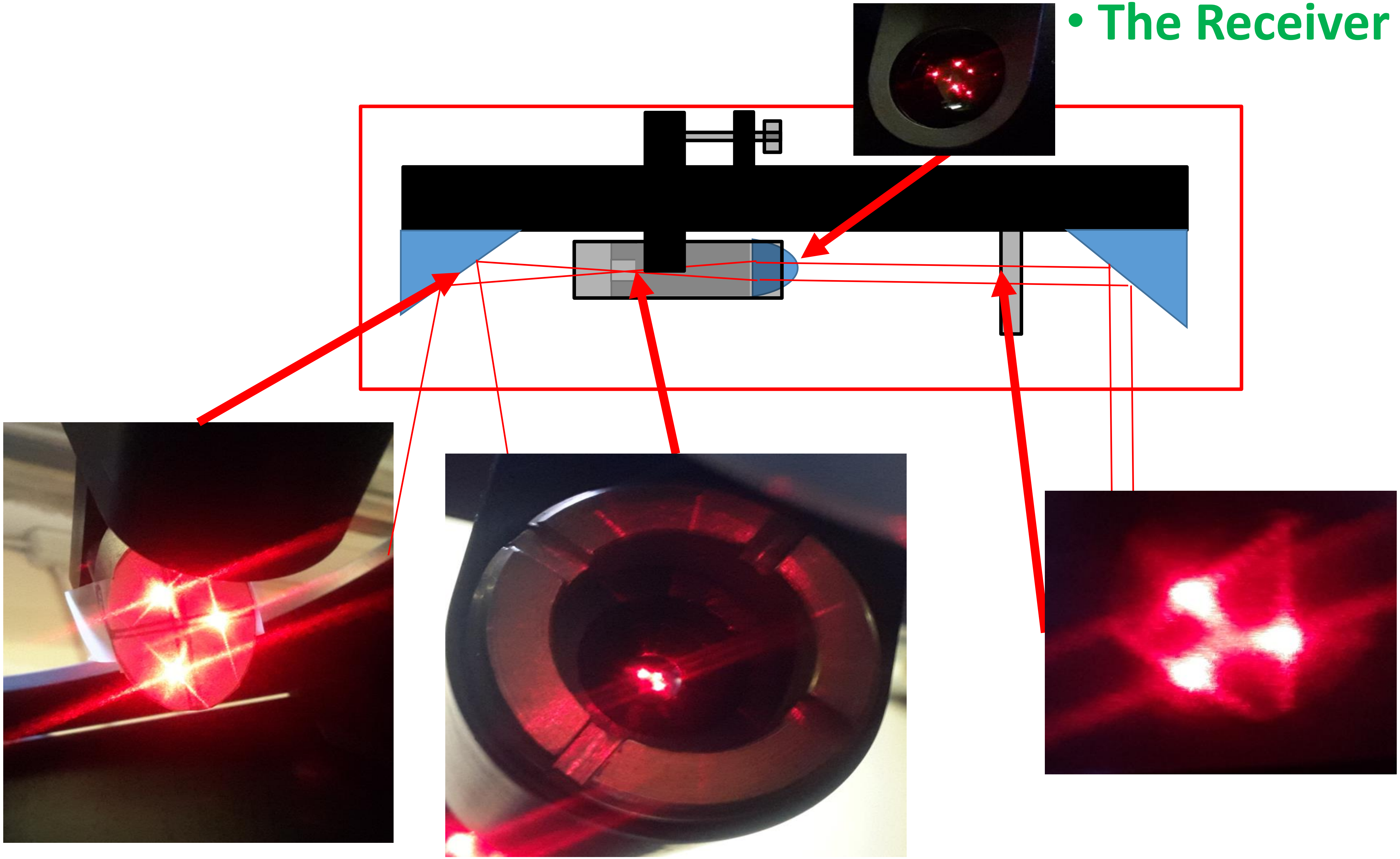

• The Receiver section

● Telescope infinity focus position

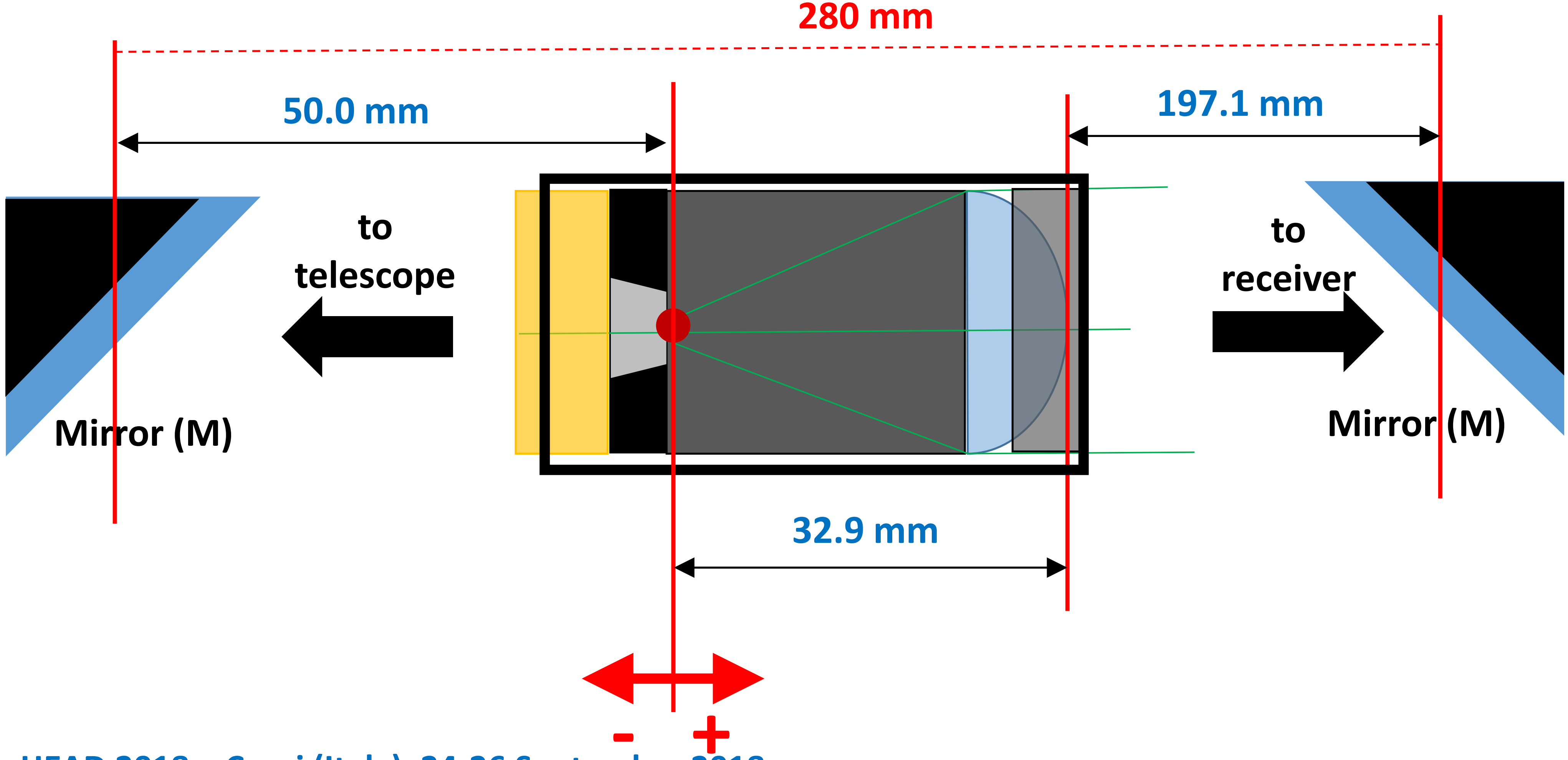

raw indetermination
± 0.2 mm

280 mm

50.0 mm

197.1 mm

to
telescope

to
receiver

Mirror (M)

Mirror (M)

32.9 mm

\-

\+

ZEMAX© simulation

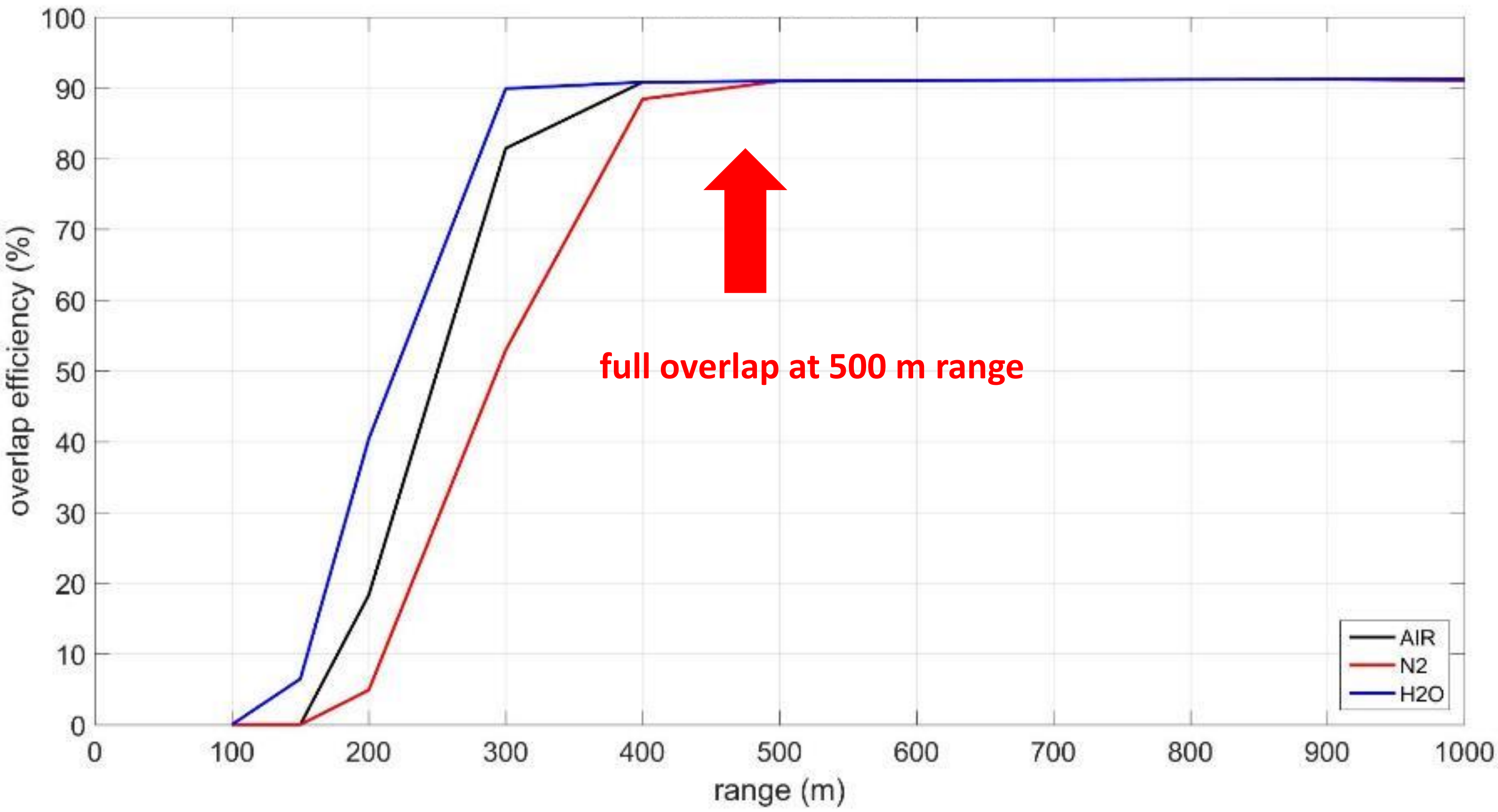

full overlap at 500 m range

Receiver spectral efficiencies measurements

- **The Receiver section**

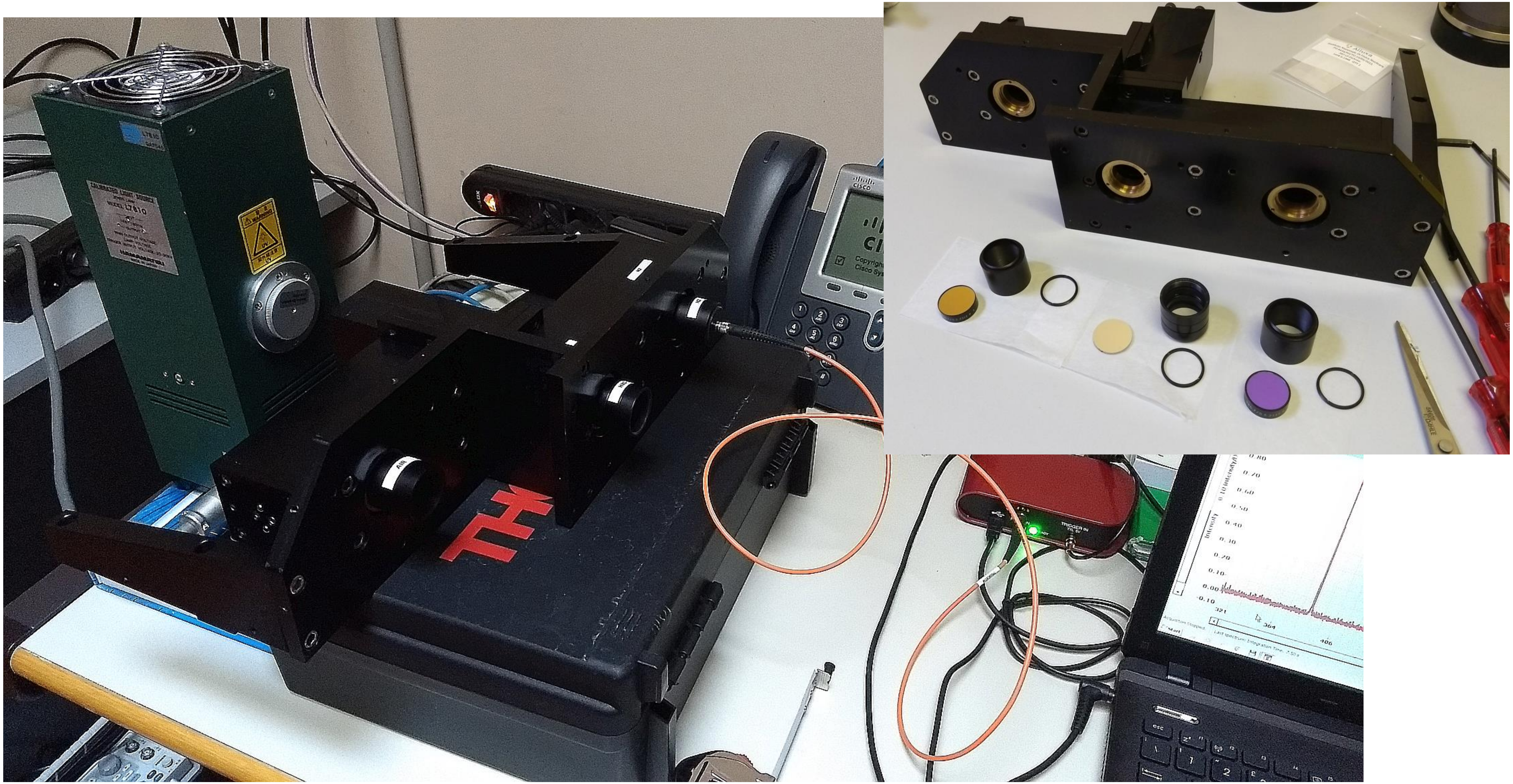

- The Receiver section

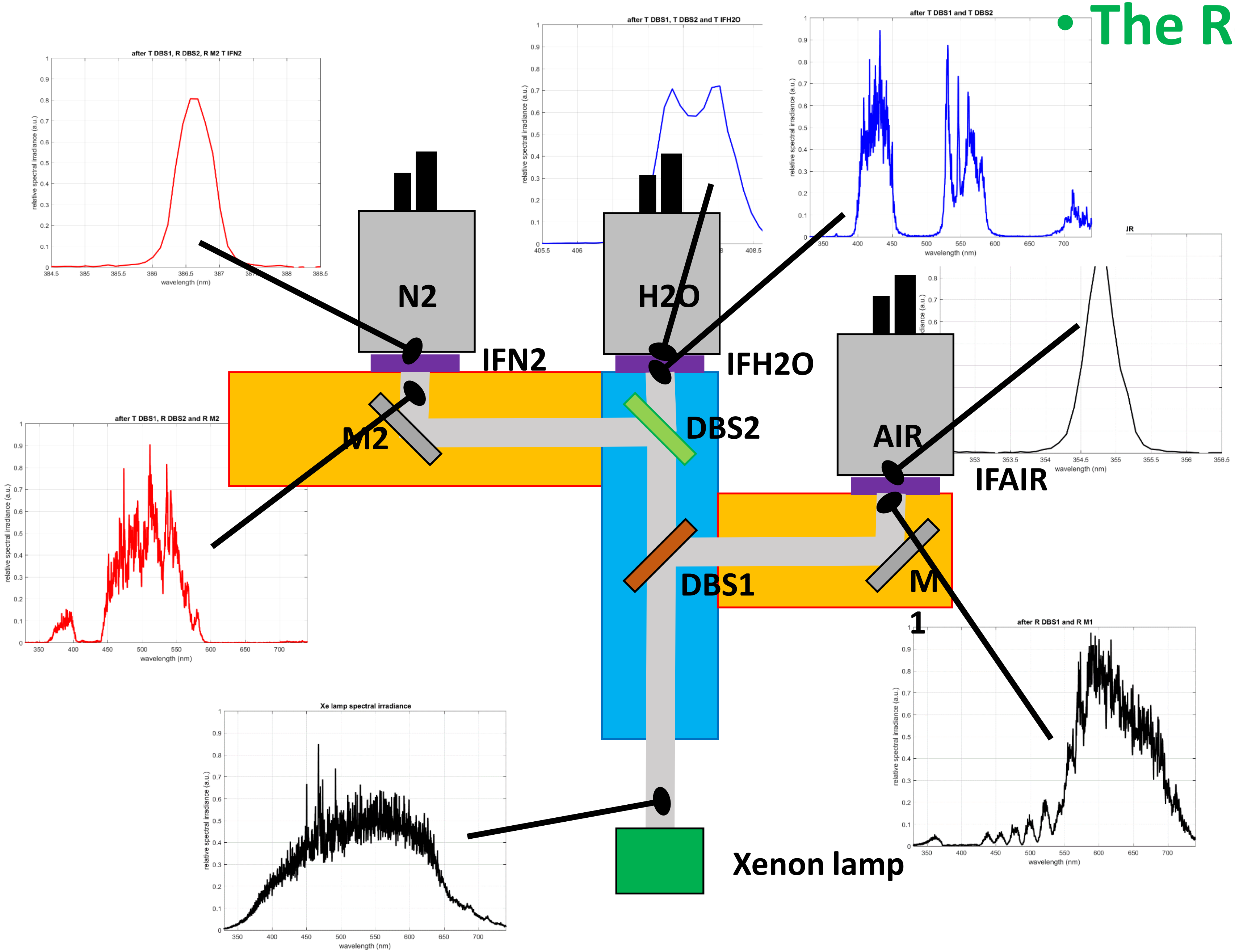

• The Receiver section

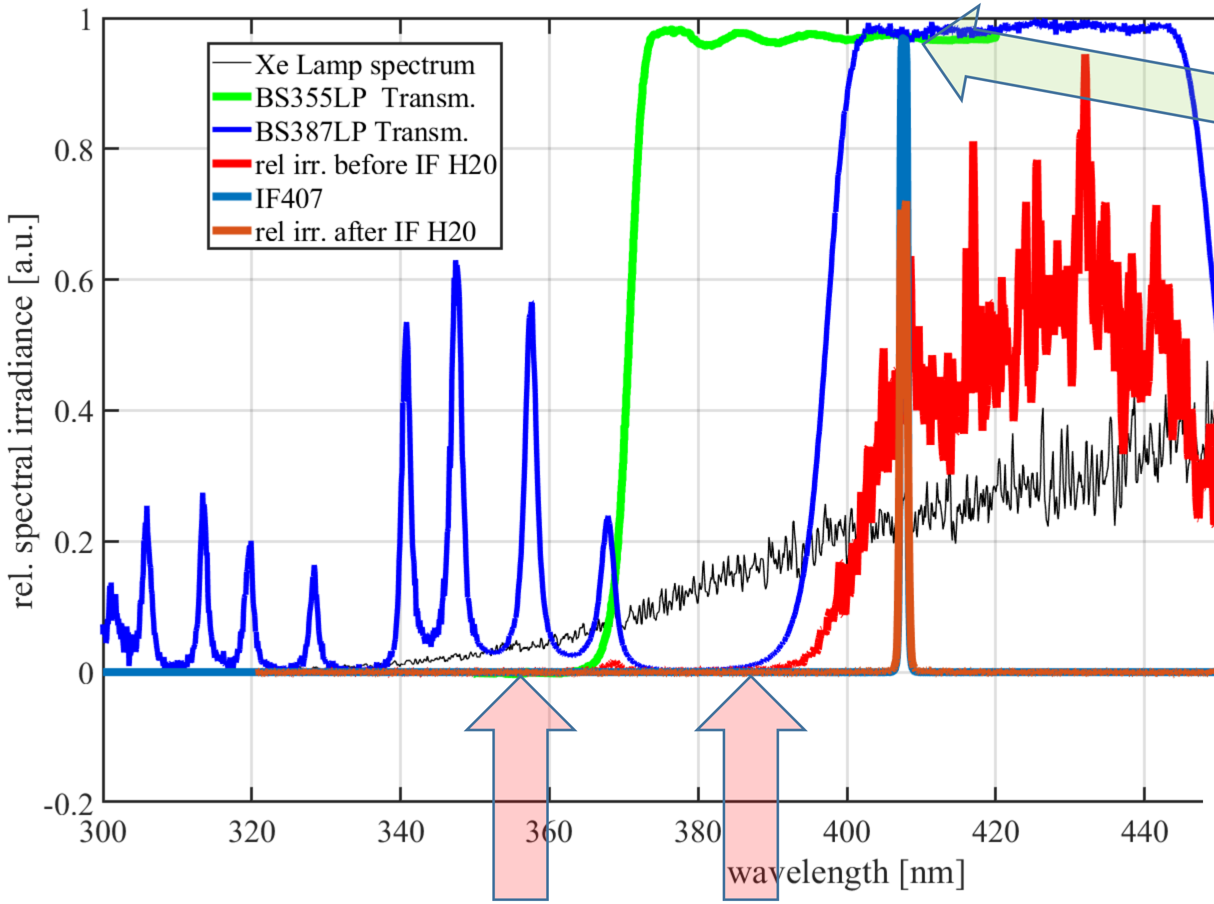

Both the DBS transmits almost all the H20 Raman signal

The AIR and the N2 signal are efficiently removed by the DBS and after the IF407 no significant residual unwanted light are present.

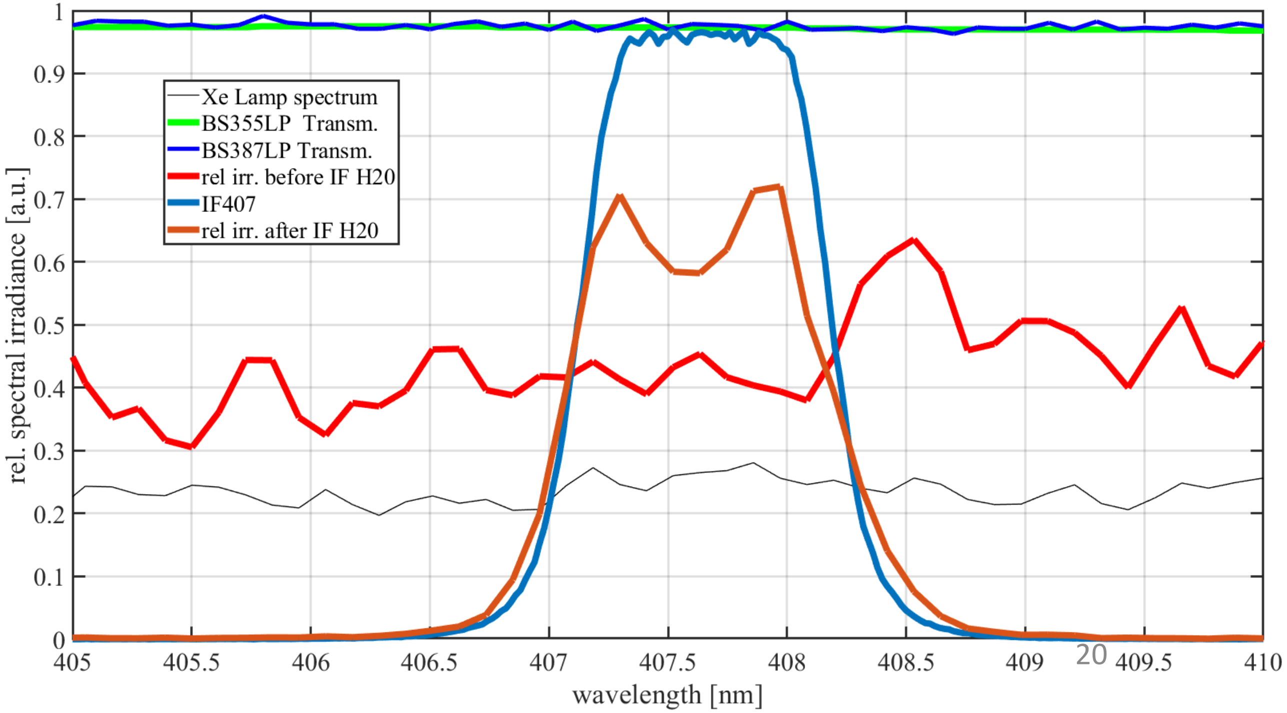

- The Receiver section

IFAIR interference filter air 354.7/0.5 nm

specifications

transmission

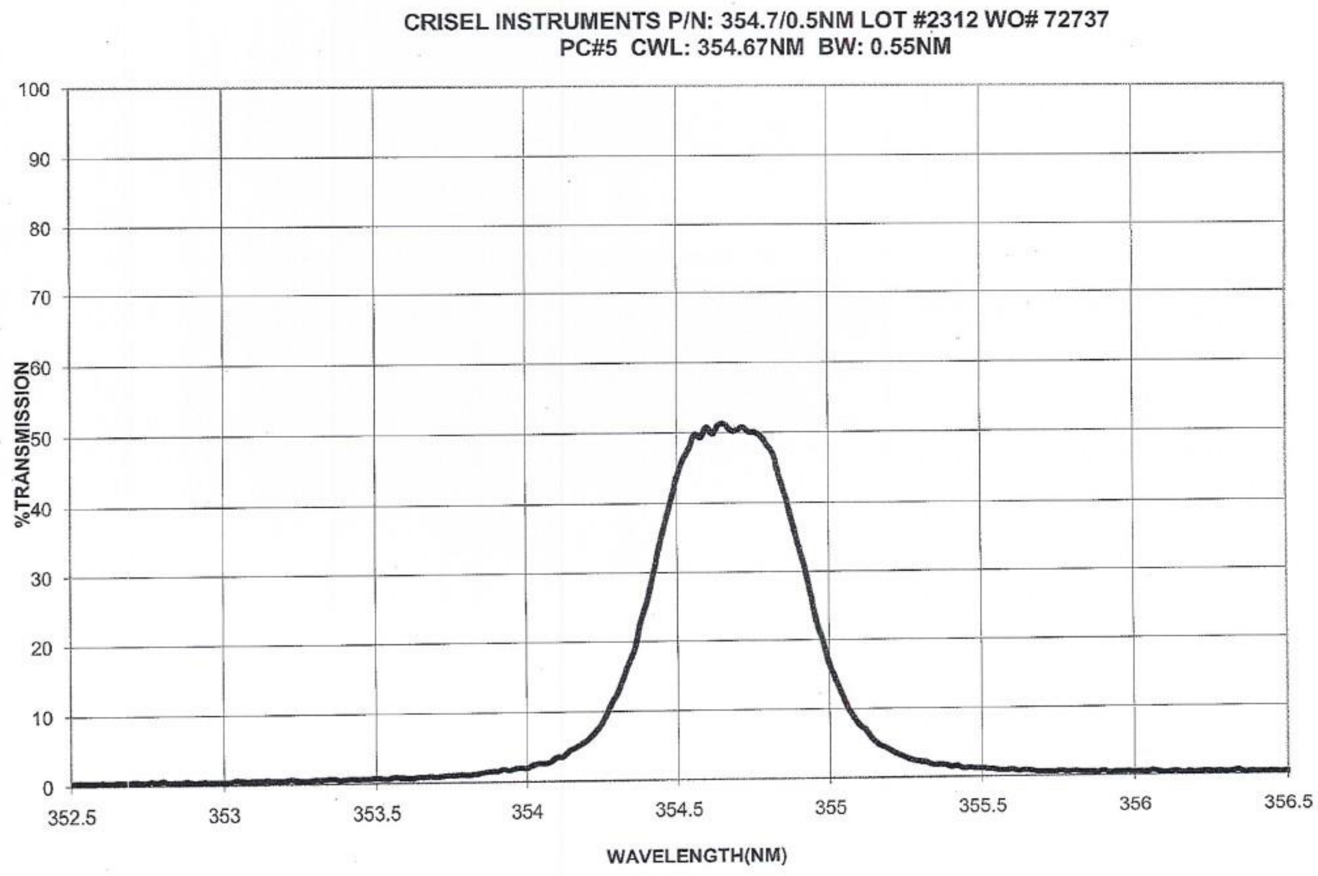
CRISEL INSTRUMENTS P/N: 354.7/0.5NM LOT #2312 WO# 72737
PC#5 CWL: 354.67NM BW: 0.55NM

optical depth

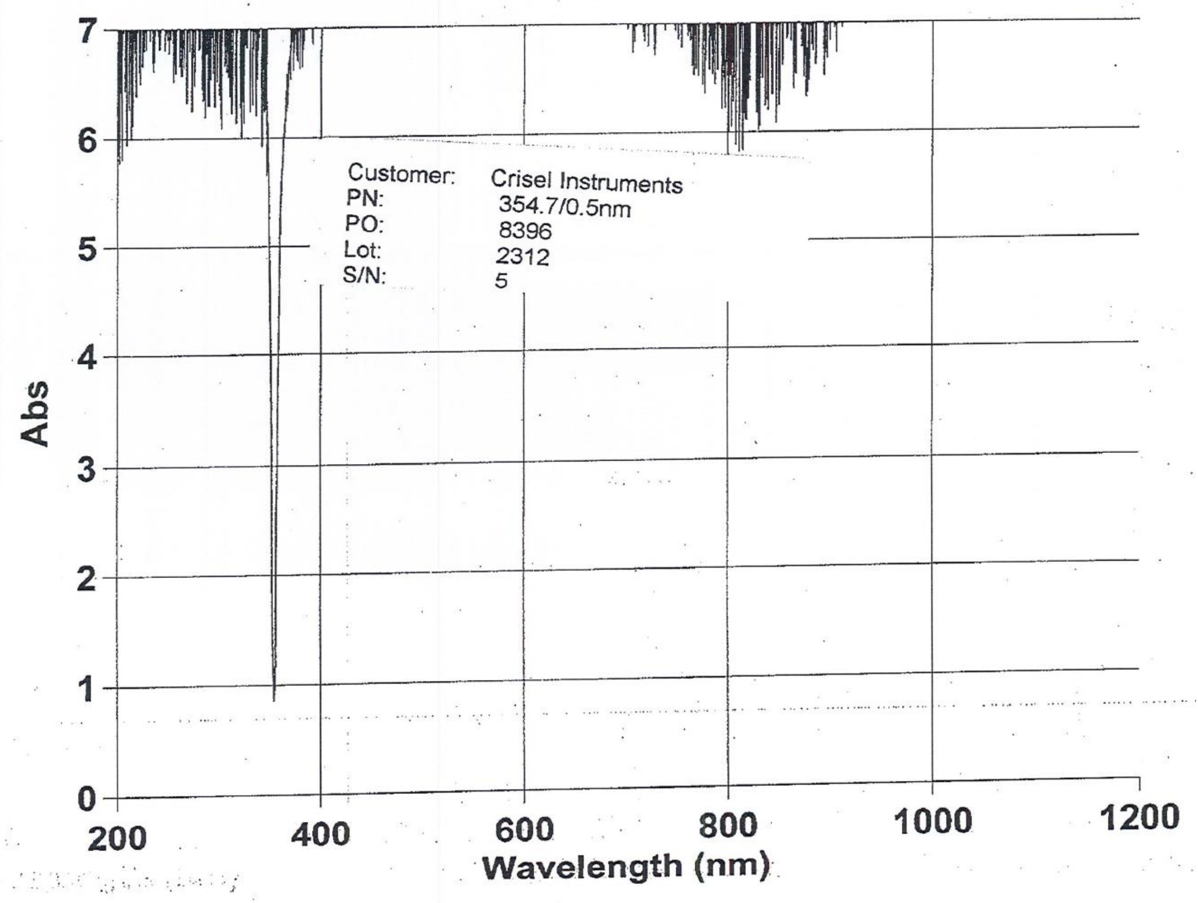
Customer: Crisel Instruments
PN: 354.7/0.5nm
PO: 8396
Lot: 2312
S/N: 5

Spectra efficiencies simulation of receiver

- The Receiver section

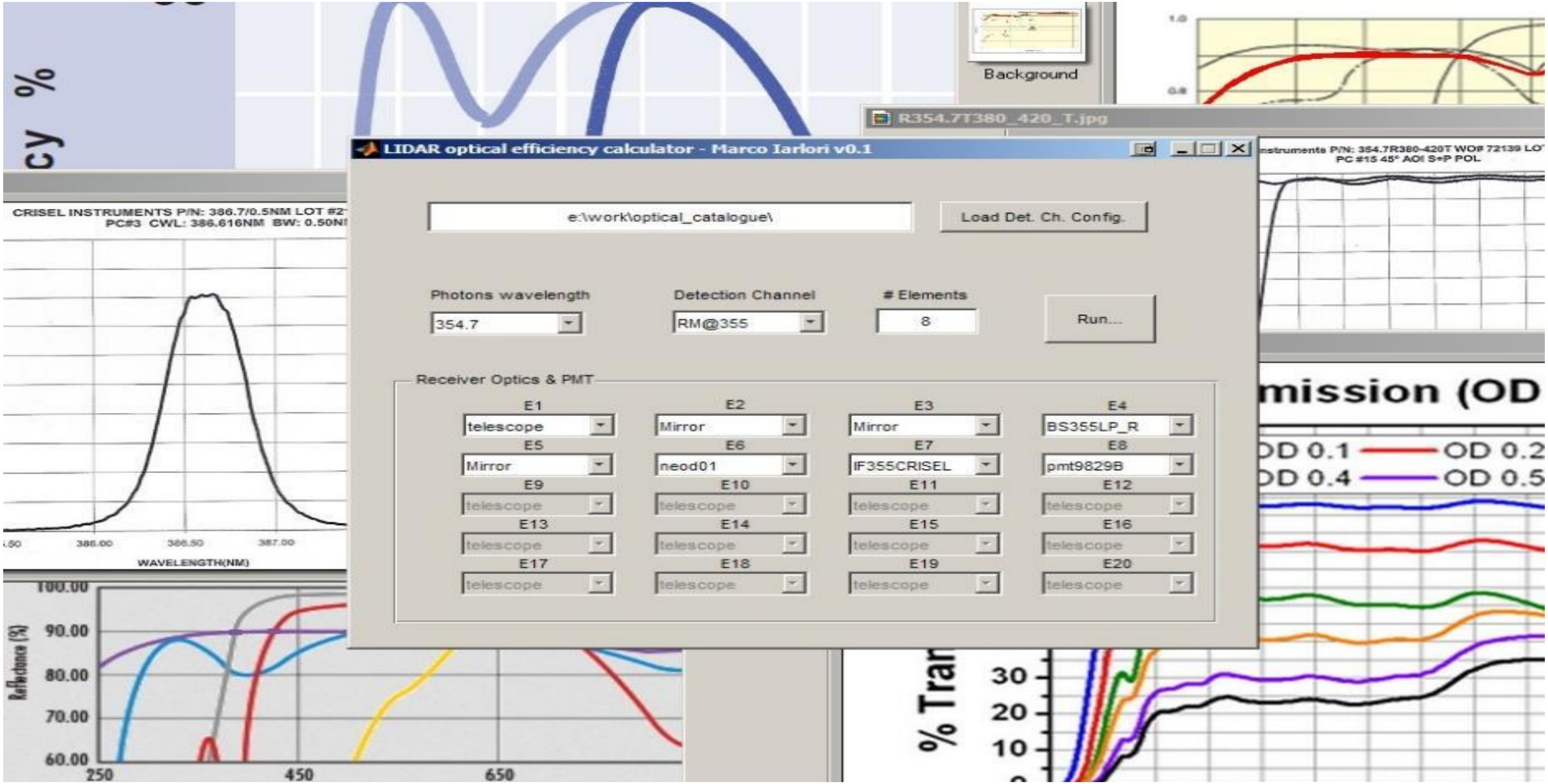

e:\work\optical_catalogue\

Photons wavelength: 354.7

Detection Channel: RM@355

Elements: 8

Receiver Optics & PMT

E1	E2	E3	E4
telescope	Mirror	Mirror	BS355LP_R
E5	**E6**	**E7**	**E8**
Mirror	neod01	IF355CRISEL	pmt9829B
E9	**E10**	**E11**	**E12**
telescope	telescope	telescope	telescope
E13	**E14**	**E15**	**E16**
telescope	telescope	telescope	telescope
E17	**E18**	**E19**	**E20**
telescope	telescope	telescope	telescope

- **The Receiver section**

Total T(%) in the RM@355 channel = 9.135%

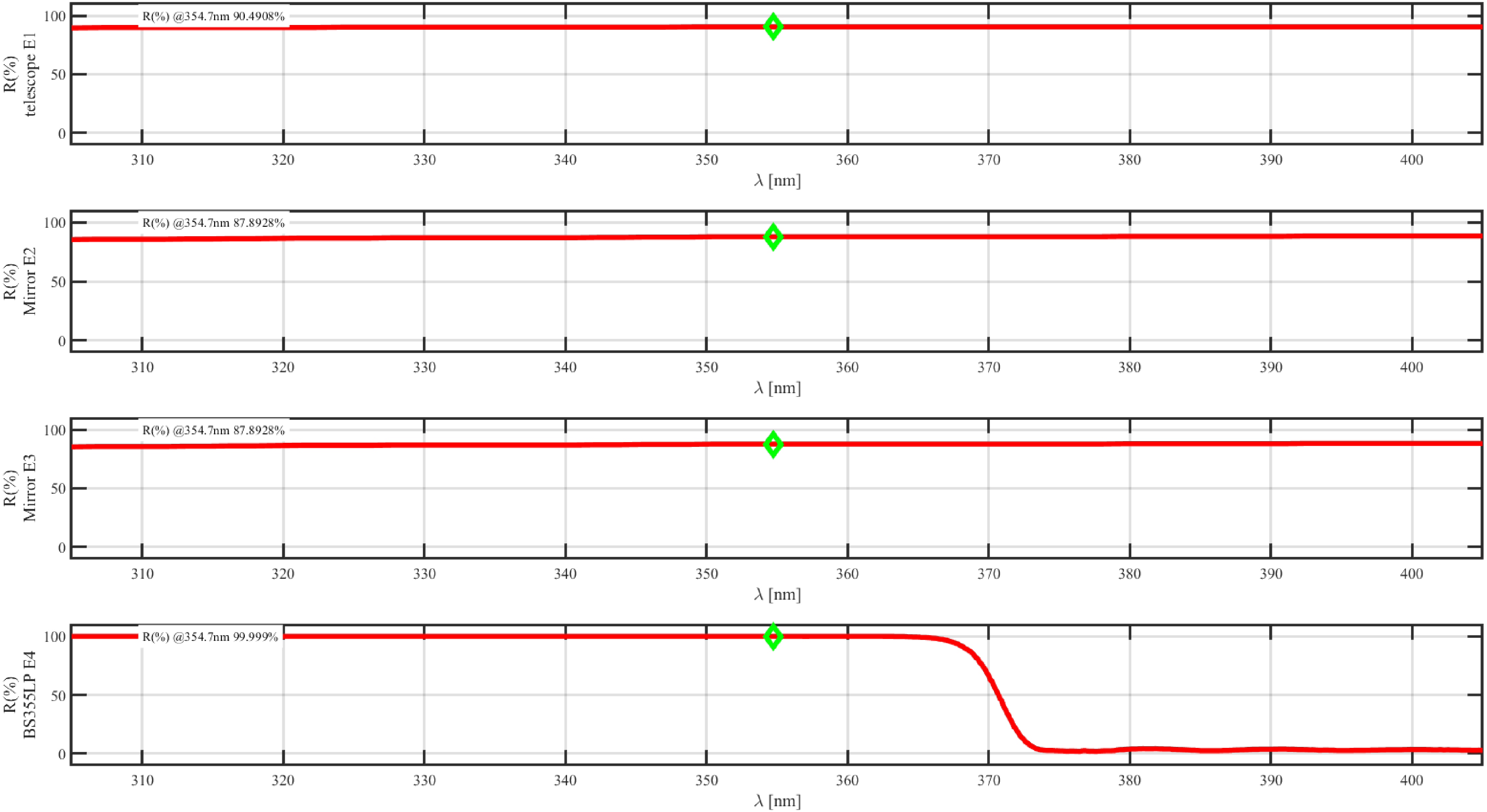

• The Receiver section

Total T(%) in the RM@355 channel = 9.135%

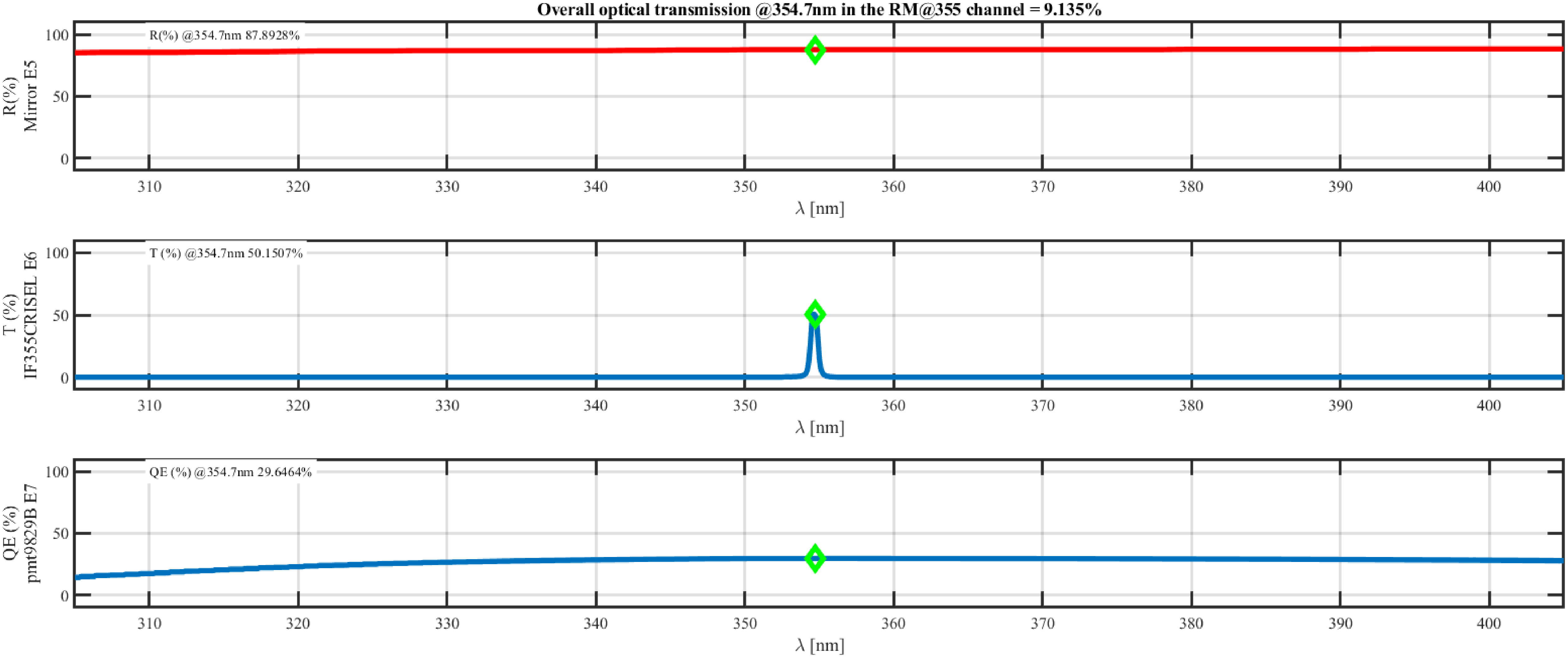

Lidar Signal simulator

- The Receiver section

LIDAR Signal Simulator (LISiSi) v0.3 - Marco Iarlori - 2017

System

Laser Wavelength (nm): 355

3 Pulse Energy (mJ)

0.125 Telescope Radius (m)

60000 # of Shots

☐ From Space?

☐ From Airplane?

☑ radiosonde

☐ No background

☐ No noise

Aerosol Parameters (extinction and lidar ratio @355nm)

☑ PBL

1 PBL height (km)

2e-4 Max ext. (m-1)

50 Lidar Ratio (sr)

Erf Shape

1 Aexpo UV-VIS

1 Aexpo VIS-IR

1 Bexpo UV-VIS

1 Bexpo VIS-IR

☑ Aerosol Layer 1

4 Layer start range (km)

3 Layer thickness(km)

3e-4 Max ext. (m-1)

40 Lidar Ratio (sr)

gaussian(s) Shape

0.5 Aexpo UV-VIS

1 Aexpo VIS- IR

1 Bexpo UV-VIS

1 Bexpo VIS-IR

☑ Aerosol Layer 2

10 Layer start range (km)

3 Layer thikness(km)

2e-4 Max ext. (m-1)

15 Lidar Ratio (sr)

gaussian(s) Shape

0 Aexpo UV-VIS

1 Aexpo VIS- IR

1 Bexpo UV-VIS

1 Bexpo VIS-IR

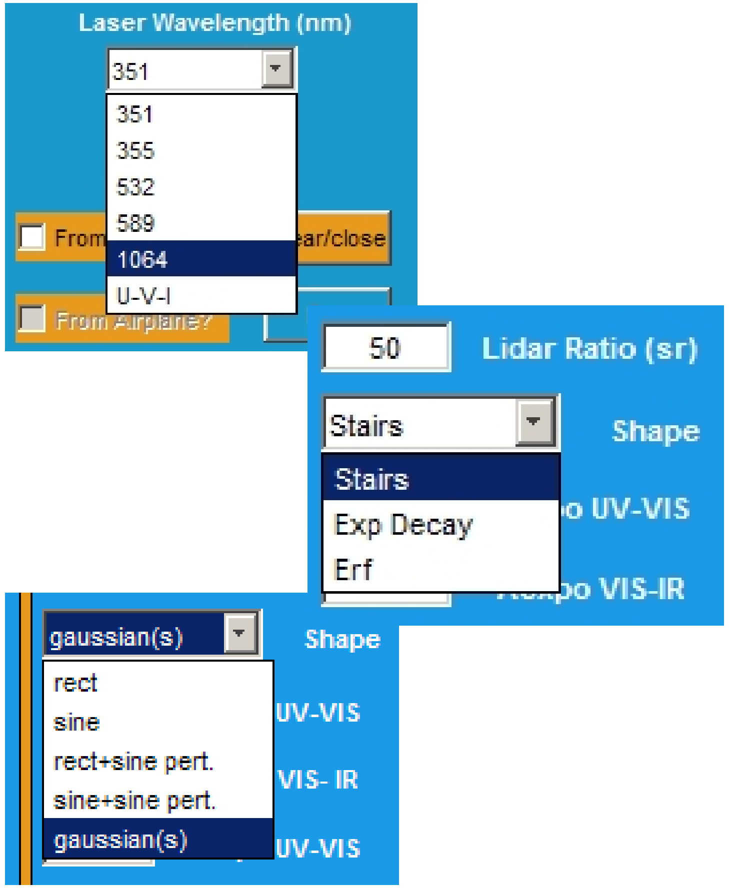

Laser Wavelength (nm): 351

50 Lidar Ratio (sr)

Stairs Shape

gaussian(s) Shape

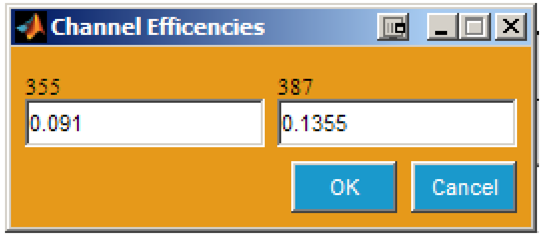

Channel Efficencies

355: 0.091

387: 0.1355

• The Receiver section

Signal Count Rate <100 MHz @ range>500m (i.e. when the estimated overlap efficiency reaches its max value) to avoid photon counting pile-up effect.

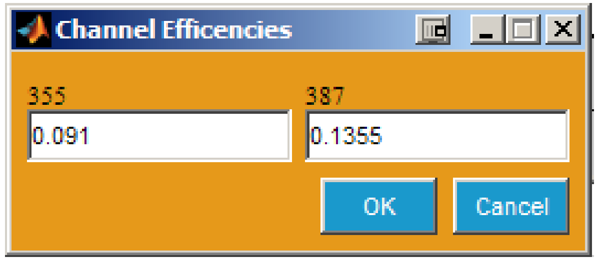

355: 0.091

387: 0.1355

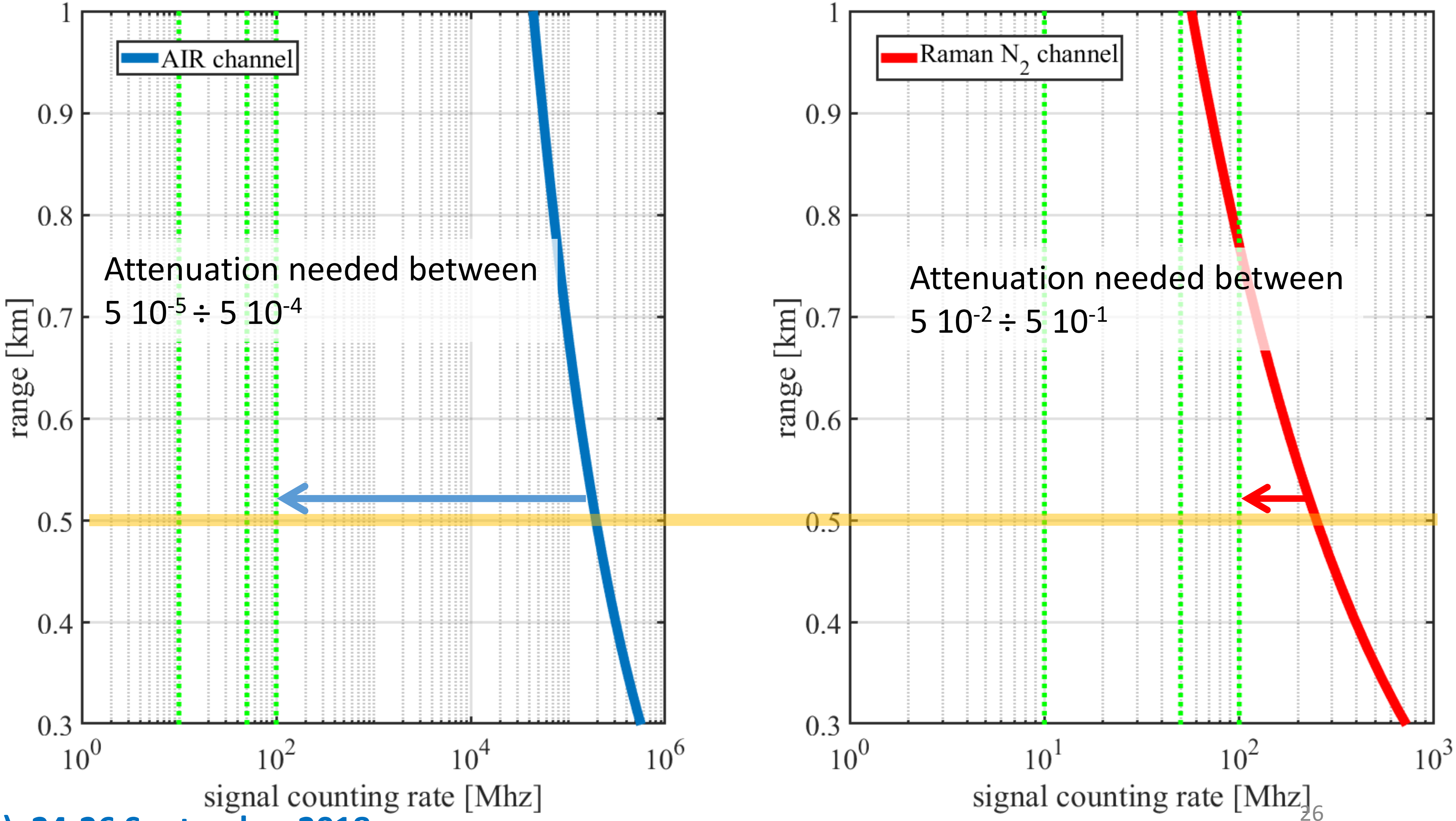

Attenuation needed between $5\ 10^{-5} \div 5\ 10^{-4}$

Attenuation needed between $5\ 10^{-2} \div 5\ 10^{-1}$

• The Receiver section

Neutral density filters

- The Receiver section

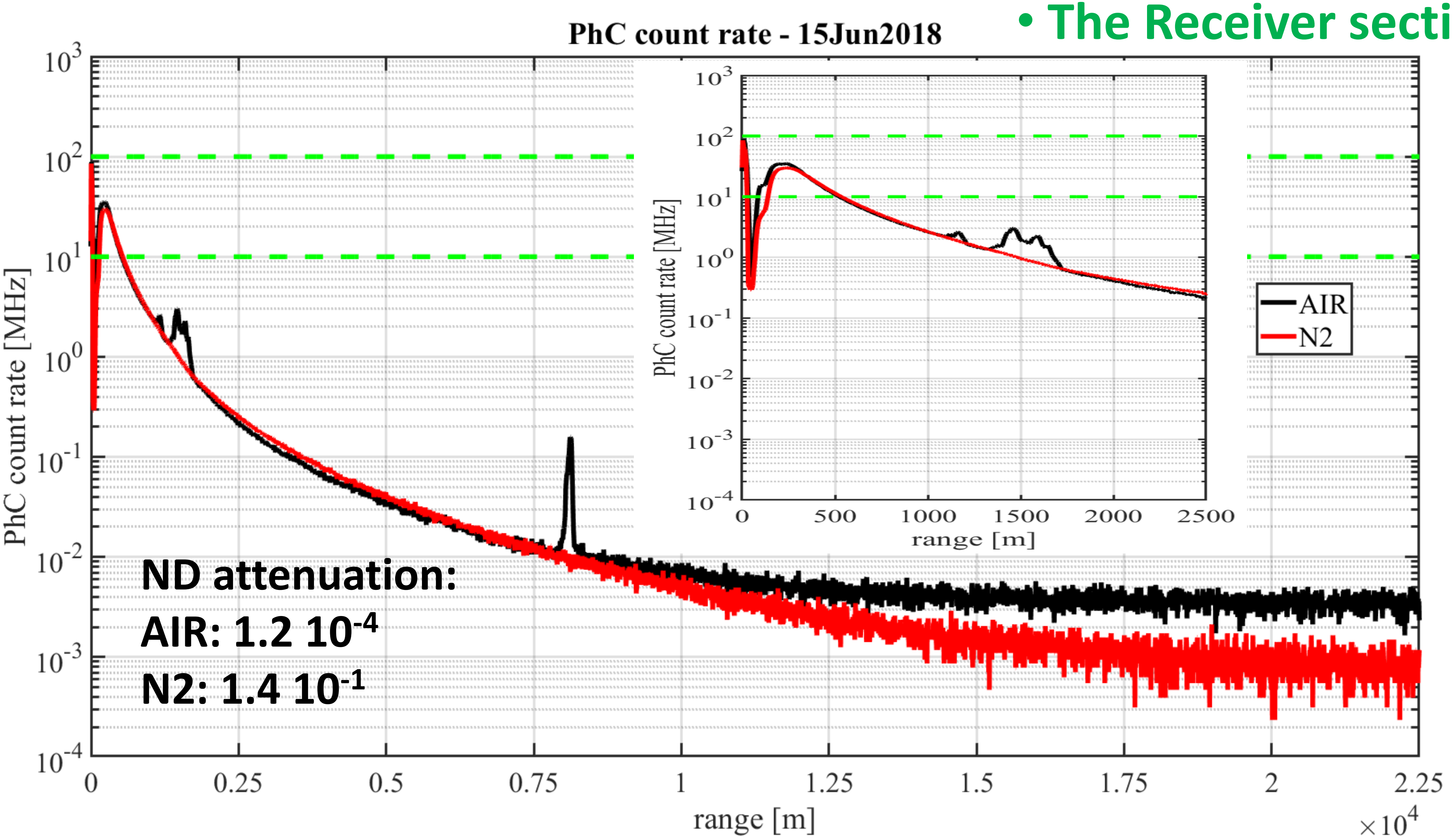

ND attenuation:

AIR: 1.2 10^{-4}

N2: 1.4 10^{-1}

photomultipliers N2/386.7 nm

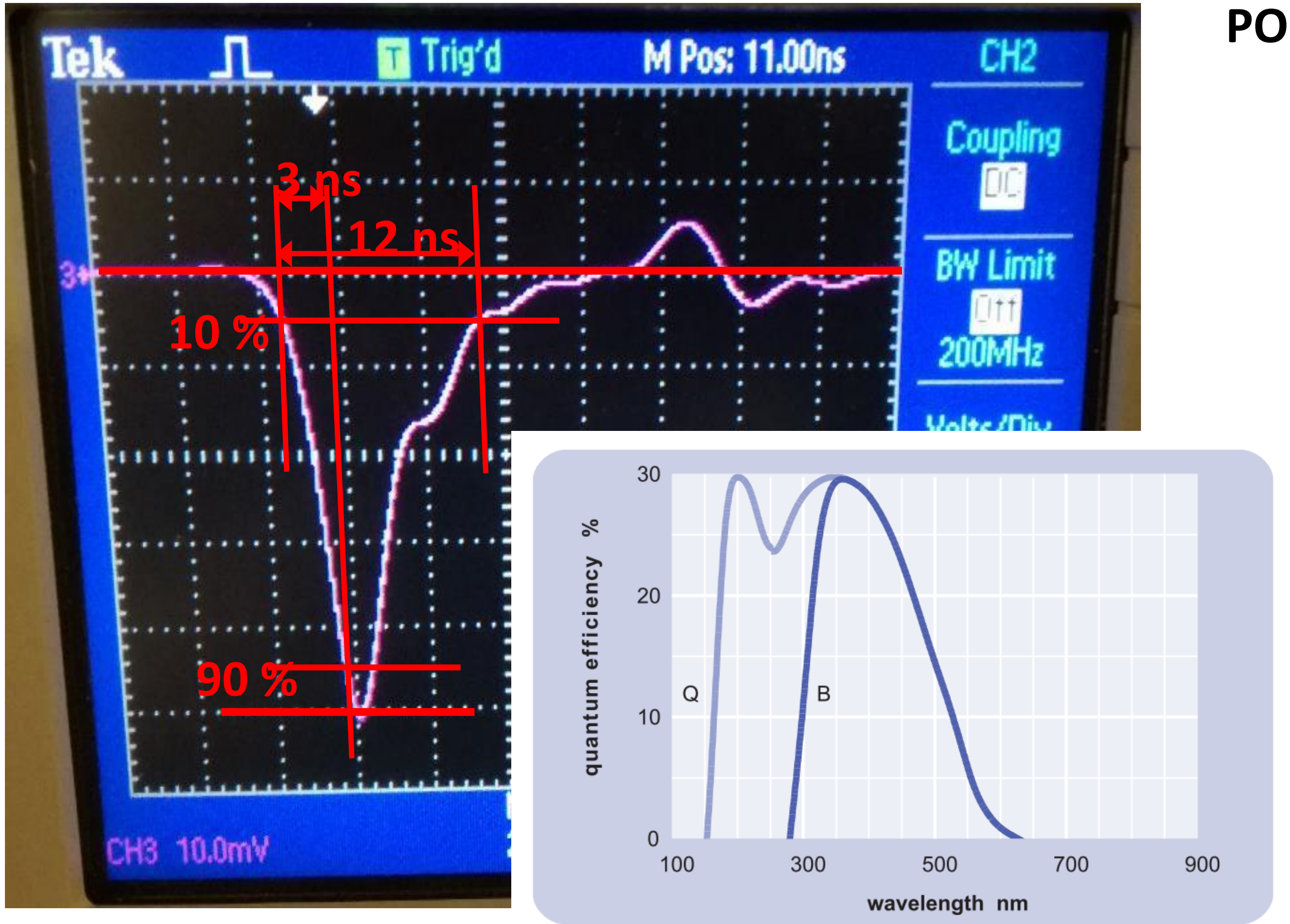

POSSIBLE SETUP OF PMTs'HV and threshold signal level

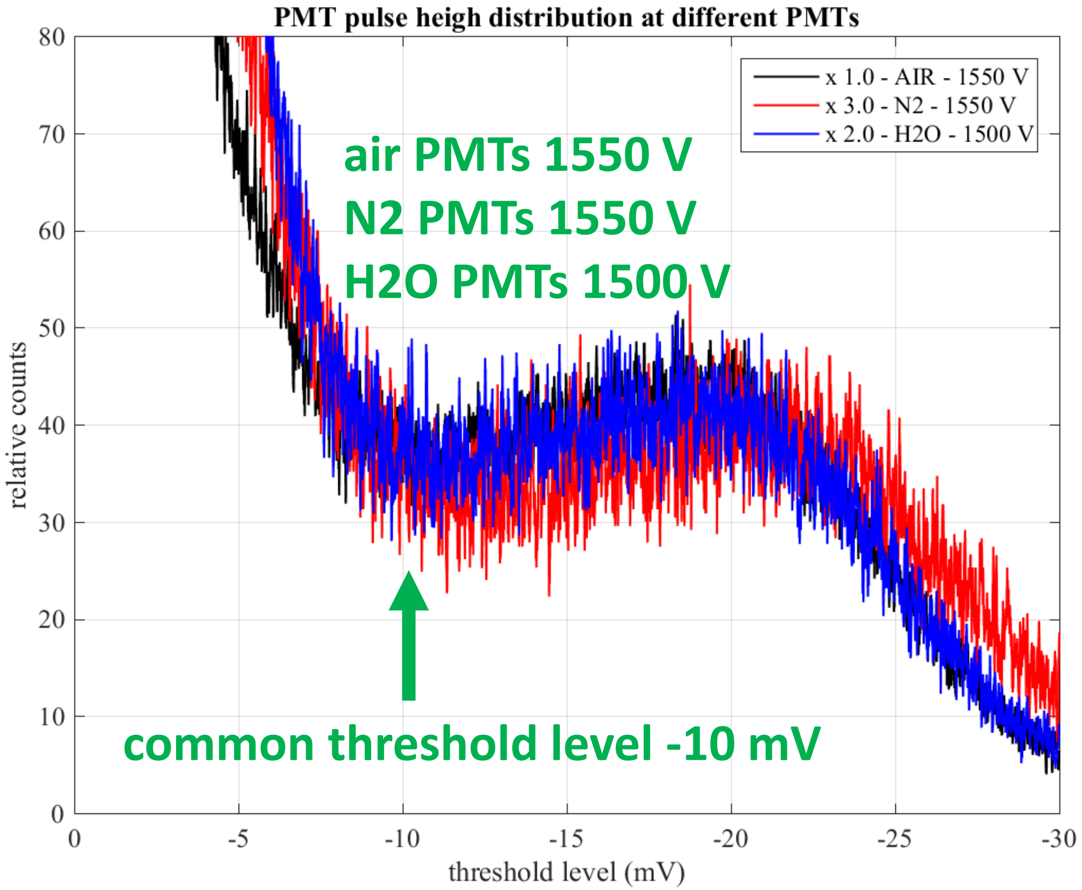

air PMTs 1550 V

N2 PMTs 1550 V

H2O PMTs 1500 V

common threshold level -10 mV

51 mm (2") photomultiplier

ET 9829QB -> QE% optimized for the UV

• The Receiver section

TIMING MEASUREMENTS for «zero-bin» estimation.

MEASUREMENTS WITH FAST PHOTODIODE
of the laser emission at laser exit

MEASUREMENTS WITH OSCILLOSCOPE
of the local reflection/echoes

MEASUREMENTS WITH APC26-DAQs
of the local reflection/echoes

«zero-bin»: the assumed zero range of the signal recording.
A non accurate measurements can cause large errors in the AE and AOD.
V. Freudenthaler, et al., Atmos. Meas. Tech. Discuss.,https://doi.org/10.5194/amt-2017-395.

To reduce the «zero bin» indetermination even the smallest sources of delays must be taken into account.

- **The Receiver section**

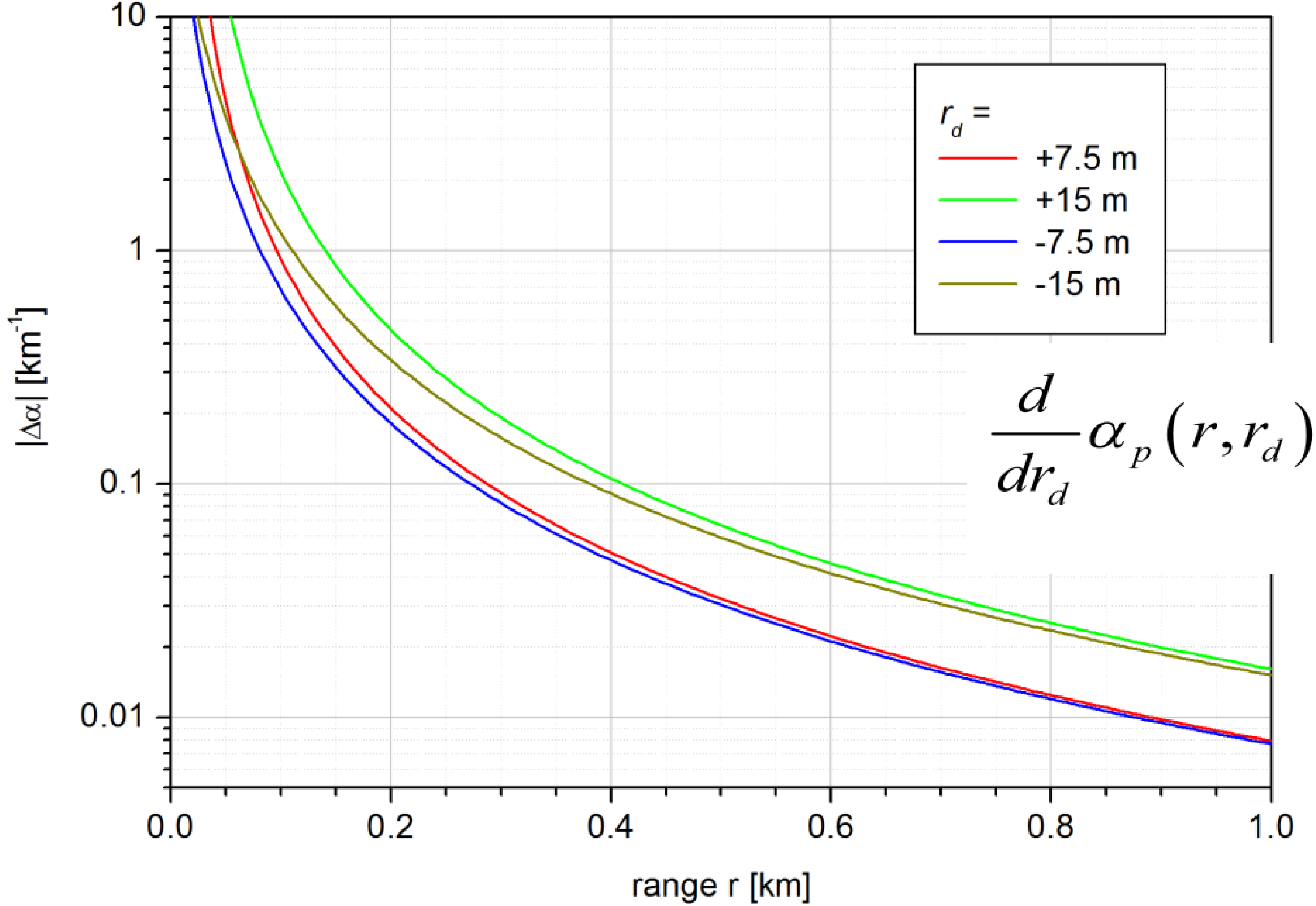

$$\frac{d}{dr_d}\alpha_p\left(r,r_d\right)\approx-\frac{2}{1+f_p}\frac{1}{\left(r-r_d\right)^2}$$

• The Receiver section

SUMMARY PhC

Q switch sync out and laser pulse emission at DAQ

MEASUREMENTS WITH FAST PHOTODIODE
of laser emission

MEASUREMENTS WITH OSCILLOSCOPE
of local reflections/echoes

MEASUREMENTS WITH APC26-DAQs
of local reflections/echoes

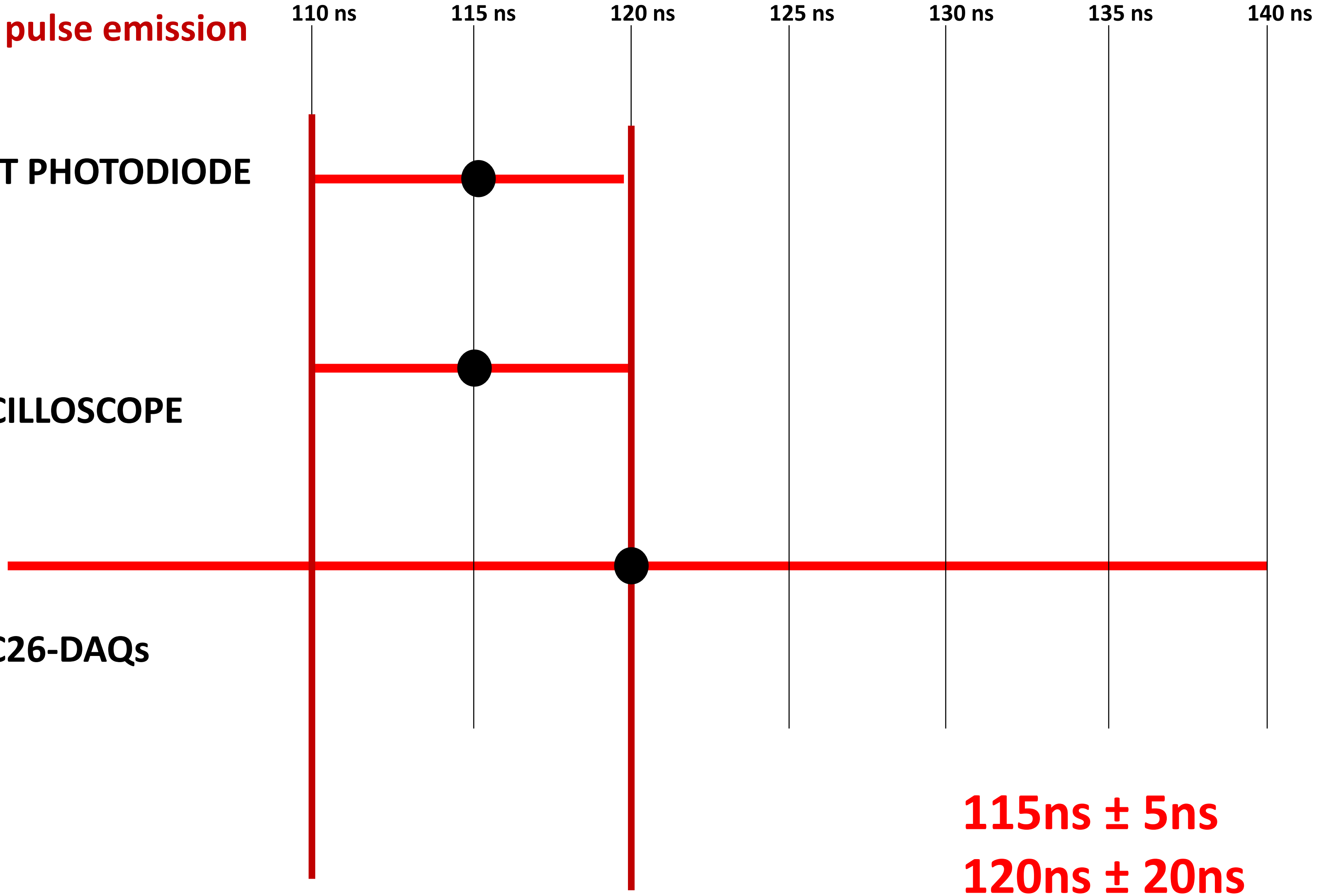

110÷120 ns

115ns ± 5ns
120ns ± 20ns

DAQ control software (developed in-house)

- **The Receiver section**

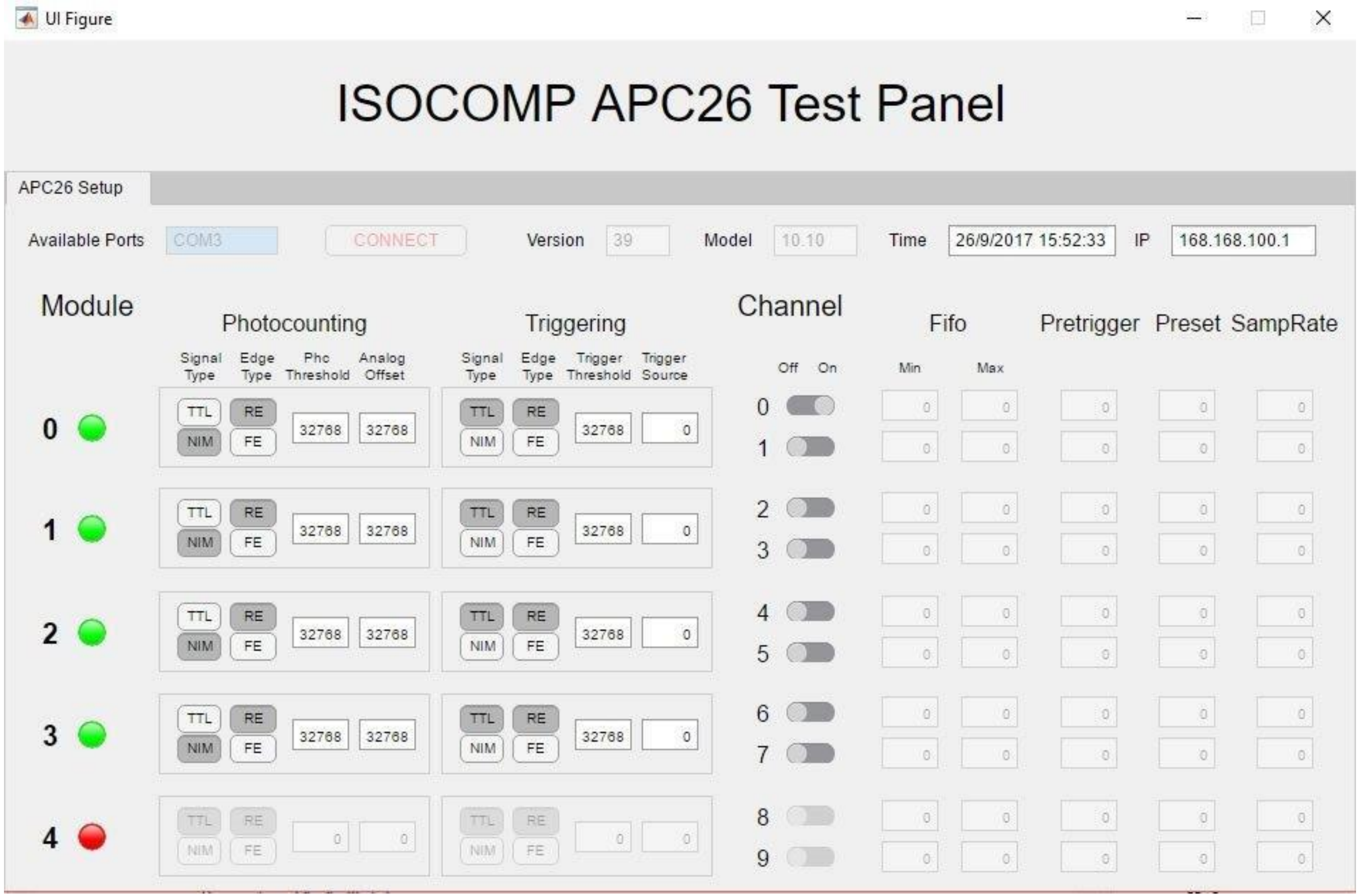

ISOCOMP APC26 Test Panel

Available Ports COM3 · Version 39 · Model 10.10 · Time 26/9/2017 15:52:33 · IP 168.168.100.1

Module	Photocounting Signal Type	Photocounting Edge Type	Phc Threshold	Analog Offset	Triggering Signal Type	Triggering Edge Type	Trigger Threshold	Trigger Source
0 ●	TTL NIM	RE FE	32768	32768	TTL NIM	RE FE	32768	0
1 ●	TTL NIM	RE FE	32768	32768	TTL NIM	RE FE	32768	0
2 ●	TTL NIM	RE FE	32768	32768	TTL NIM	RE FE	32768	0
3 ●	TTL NIM	RE FE	32768	32768	TTL NIM	RE FE	32768	0
4 ●	TTL NIM	RE FE	0	0	TTL NIM	RE FE	0	0

Channel (Off / On)	Fifo Min	Fifo Max	Pretrigger	Preset	SampRate
0	0	0	0	0	0
1	0	0	0	0	0
2	0	0	0	0	0
3	0	0	0	0	0
4	0	0	0	0	0
5	0	0	0	0	0
6	0	0	0	0	0
7	0	0	0	0	0
8	0	0	0	0	0
9	0	0	0	0	0

The DAQ control (command-line version) enables to:

- **open/close the dome;**
- **control the altazimuth movements;**
- **read the weather station data;**
- **power up/starts all the lidar hardware;**
- **start/stop the acquisition accordingly to the ORM policy;**
- **shutdown the system in emergency situation;**
- **process the data analysis.**

•Aerosol & Water Vapor profiles

$$P_{\lambda_0}(z) = K_{\lambda_0} \frac{O(z)}{z^2} [\beta_{\lambda_0}{}^{\text{aer}}(z) + \beta_{\lambda_0}{}^{\text{mol}}(z)] \times \exp\left\{-2 \int_0^z [\alpha_{\lambda_0}{}^{\text{aer}}(\zeta) + \alpha_{\lambda_0}{}^{\text{mol}}(\zeta)] \mathrm{d}\zeta\right\}$$

Elastic lidar EQ

Raman lidar EQ

$$P_{\lambda_R}(z) = K_{\lambda_R} \frac{O(z)}{z^2} N_R(z) \frac{\mathrm{d}\sigma_{\lambda_R}(\pi)}{\mathrm{d}\Omega} \times \exp\left\{- \int_0^z [\alpha_{\lambda_0}{}^{\text{mol}}(\zeta) + \alpha_{\lambda_0}{}^{\text{aer}}(\zeta) + \alpha_{\lambda_R}{}^{\text{mol}}(\zeta) + \alpha_{\lambda_R}{}^{\text{aer}}(\zeta)] \mathrm{d}\zeta\right\}.$$

•Aerosol & Water Vapor profiles

$$\alpha_{\lambda_0}{}^{\mathrm{aer}}(z) = \frac{\frac{\mathrm{d}}{\mathrm{d}z}\left[\ln \frac{N_R(z)}{P_{\lambda_R}(z)z^2}\right] - \alpha_{\lambda_0}{}^{\mathrm{mol}}(z) - \alpha_{\lambda_R}{}^{\mathrm{mol}}(z)}{1 + \left(\frac{\lambda_0}{\lambda_R}\right)^k}$$

Aerosol extinction (from N_2 signal)

$$\beta_{\lambda_0}{}^{\mathrm{aer}}(z) = -\beta_{\lambda_0}{}^{\mathrm{mol}}(z) + [\beta_{\lambda_0}{}^{\mathrm{aer}}(z_0) + \beta_{\lambda_0}{}^{\mathrm{mol}}(z_0)] \times \frac{P_{\lambda_R}(z_0)P_{\lambda_0}(z)N_R(z)}{P_{\lambda_0}(z_0)P_{\lambda_R}(z)N_R(z_0)} \times \frac{\exp\left\{-\int_{z_0}^{z}[\alpha_{\lambda_R}{}^{\mathrm{aer}}(\zeta) + \alpha_{\lambda_R}{}^{\mathrm{mol}}(\zeta)]\mathrm{d}\zeta\right\}}{\exp\left\{-\int_{z_0}^{z}[\alpha_{\lambda_0}{}^{\mathrm{aer}}(\zeta) + \alpha_{\lambda_0}{}^{\mathrm{mol}}(\zeta)]\mathrm{d}\zeta\right\}}.$$

Aerosol backscatter (from AIR & N_2 signal)

•Aerosol & Water Vapor profiles

AOD
From N_2 signal

$$\tau_{aer}(z) = -\frac{log\left(\frac{K_{\lambda_R} z^2 P_{\lambda_R}(z)}{T_{mol,\lambda_0}(z) T_{mol,\lambda_R}(z) N_R(z)}\right)}{1+\left(\frac{\lambda_o}{\lambda_R}\right)^k}$$

$$T_{mol,\lambda}(z) = exp\left(-\int_{z_0}^{z} \alpha_{mol,\lambda}(\zeta)\, d\zeta\right)$$

OR…

$$\tau_{aer}(z)= \int_{z_0}^{z} \alpha_{aer,\lambda_0}(\zeta)\, d\zeta$$

•Aerosol & Water Vapor profiles

Water Vapor mixing ratio (g/kg)
From H_2O & N_2 signal

$$m_{\mathrm{H_2O}} = \frac{\rho_{\mathrm{H_2O}}(z)}{\rho_{\mathrm{air}}(z)} \sim \frac{N_{\mathrm{H_2O}}(z)}{N_{\mathrm{N_2}}(z)}$$

$$m_{\mathrm{H_2O}} = \boxed{C_{\mathrm{H_2O}}} \frac{P_{\mathrm{H_2O}}(z)}{P_{\mathrm{N_2}}(z)} \frac{\exp\left[-\int_0^z \alpha_{\lambda_{\mathrm{N_2}}}(\xi)\mathrm{d}(\xi)\right]}{\exp\left[-\int_0^z \alpha_{\lambda_{\mathrm{H_2O}}}(\xi)\mathrm{d}(\xi)\right]}$$

•Aerosol & Water Vapor profiles

$$C_{\mathrm{H_2O}} = 0.7808 \frac{M_H}{M_{\mathrm{dryair}}} \frac{\frac{d\sigma_N(\pi)}{d\Omega}}{\frac{d\sigma_H(\pi)}{d\Omega}} K_{N,H}$$

$$m_{\mathrm{H_2O}} = m_{\mathrm{H_2O}}^{RAOB}$$

→

$C_{\mathrm{H_2O}}$ **Can be determined with linear regression Y=AX**

RAwinsonde OBservation (RAOB)

Linear regression C_{H2O}= 14±0.15

Stability ±0.3 (very first estimation)

•Aerosol & Water Vapor profiles

Molecular density profile

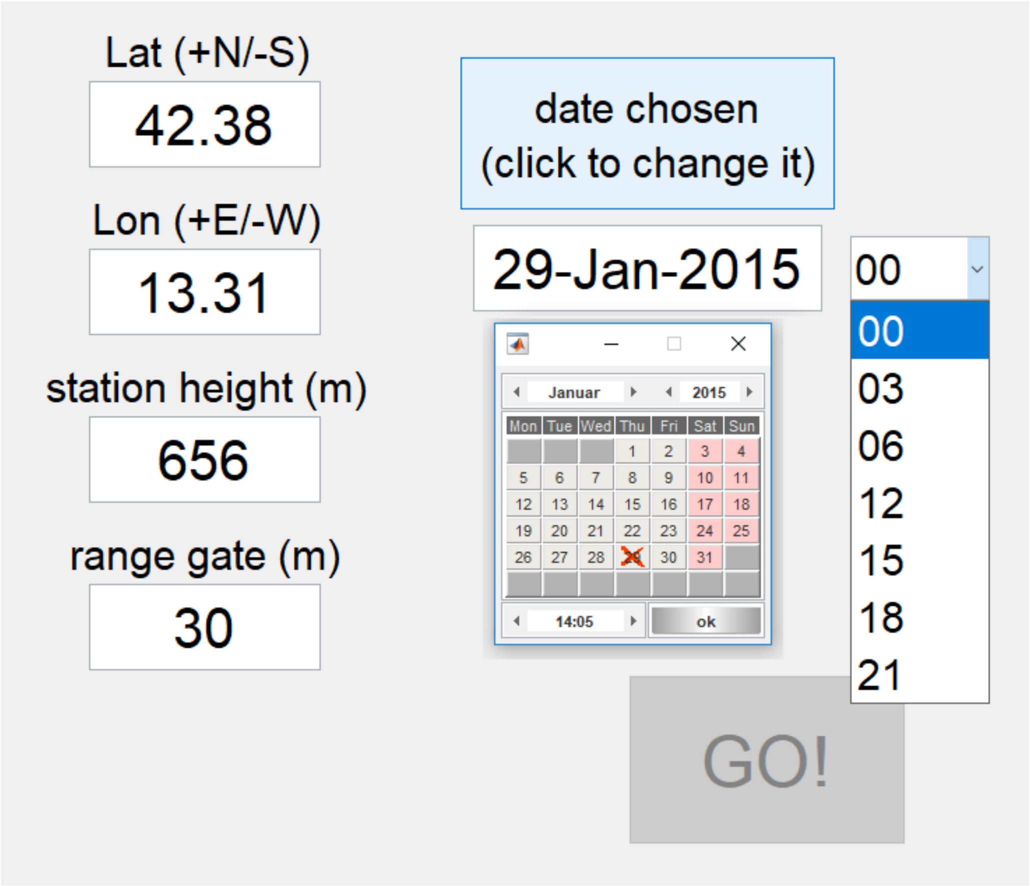

Lat (+N/-S): 42.38

Lon (+E/-W): 13.31

station height (m): 656

range gate (m): 30

29-Jan-2015

00

Mon	Tue	Wed	Thu	Fri	Sat	Sun
			1	2	3	4
5	6	7	8	9	10	11
12	13	14	15	16	17	18
19	20	21	22	23	24	25
26	27	28	29	30	31	

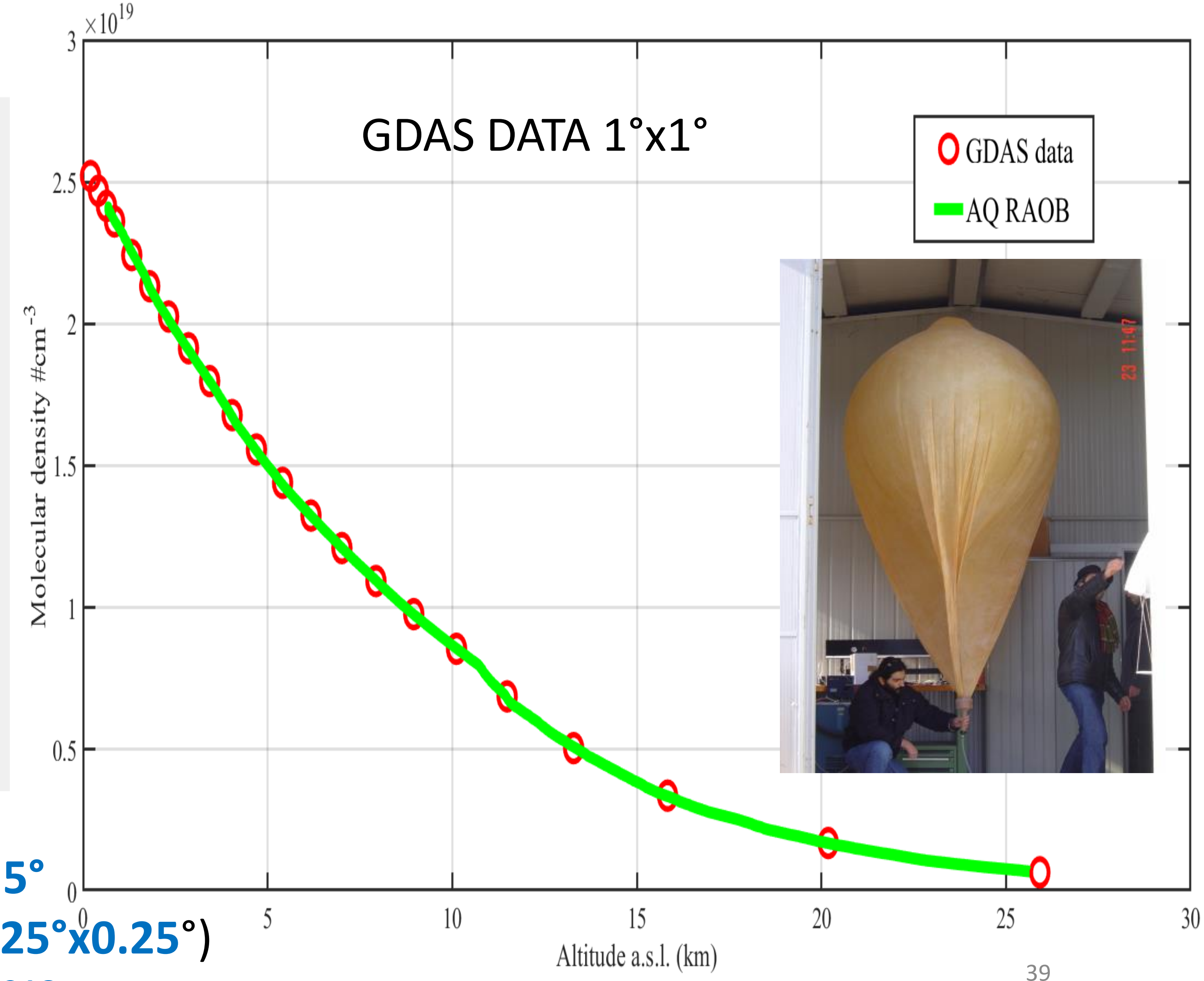

GDAS DATA 1°x1° → GDAS 0.5°x0.5°

NOW FUTURE (…or even 0.25°x0.25°)

•Aerosol & Water Vapor profiles

AIR SIGNAL 6-7 june 2018

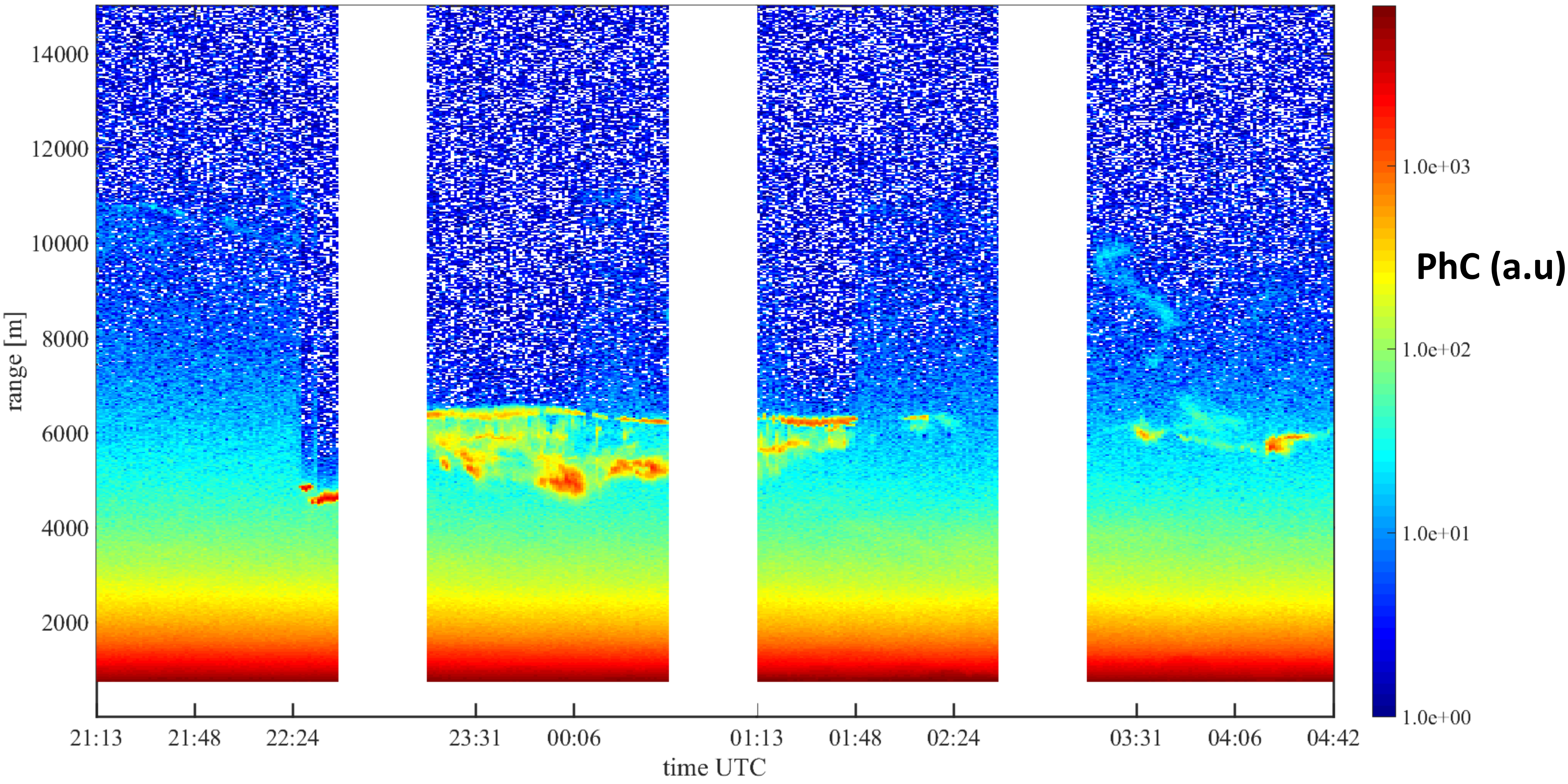

Rayleigh Fit

- **Aerosol & Water Vapor profiles**

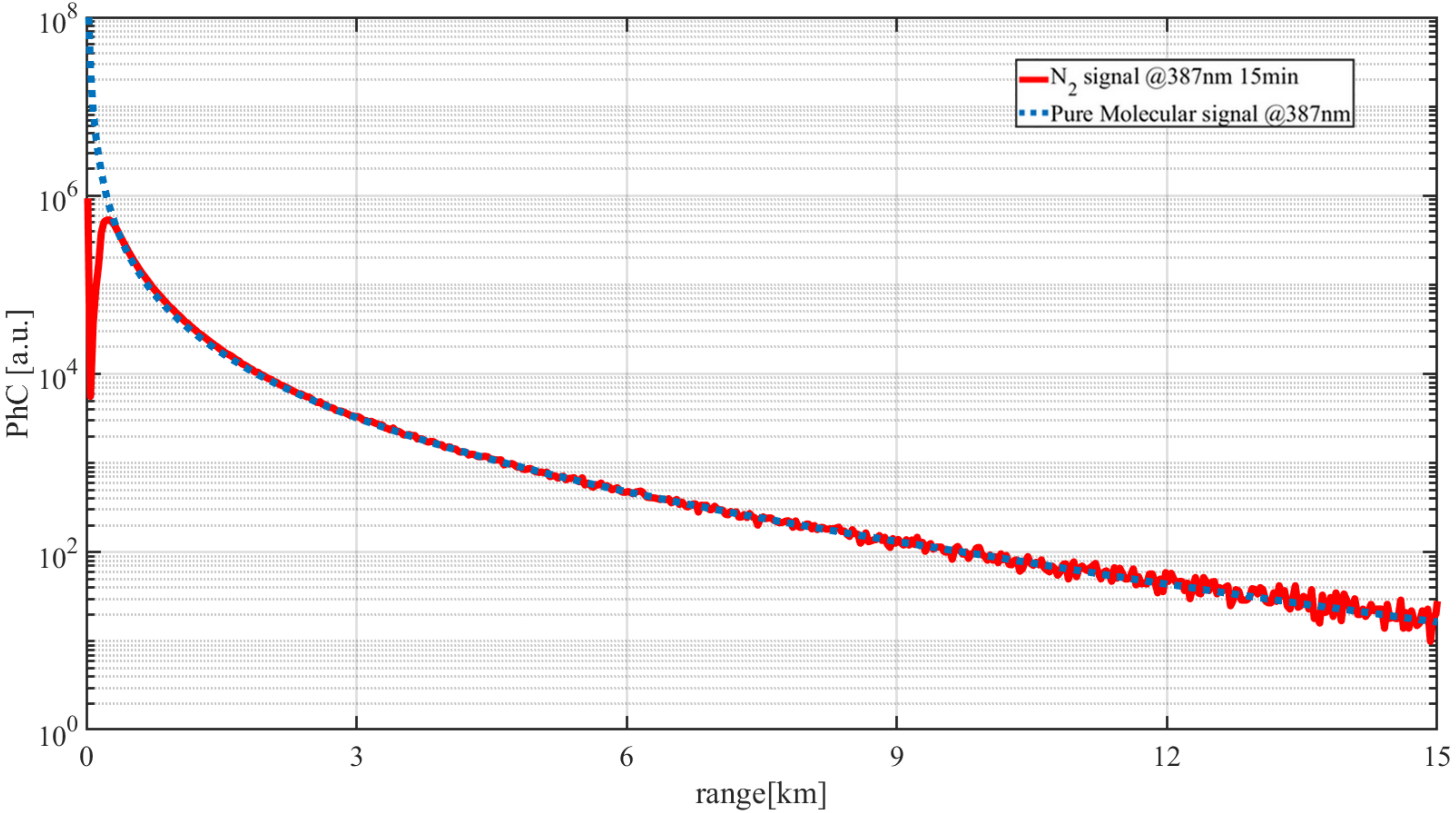

15 june 2018

•Aerosol & Water Vapor profiles

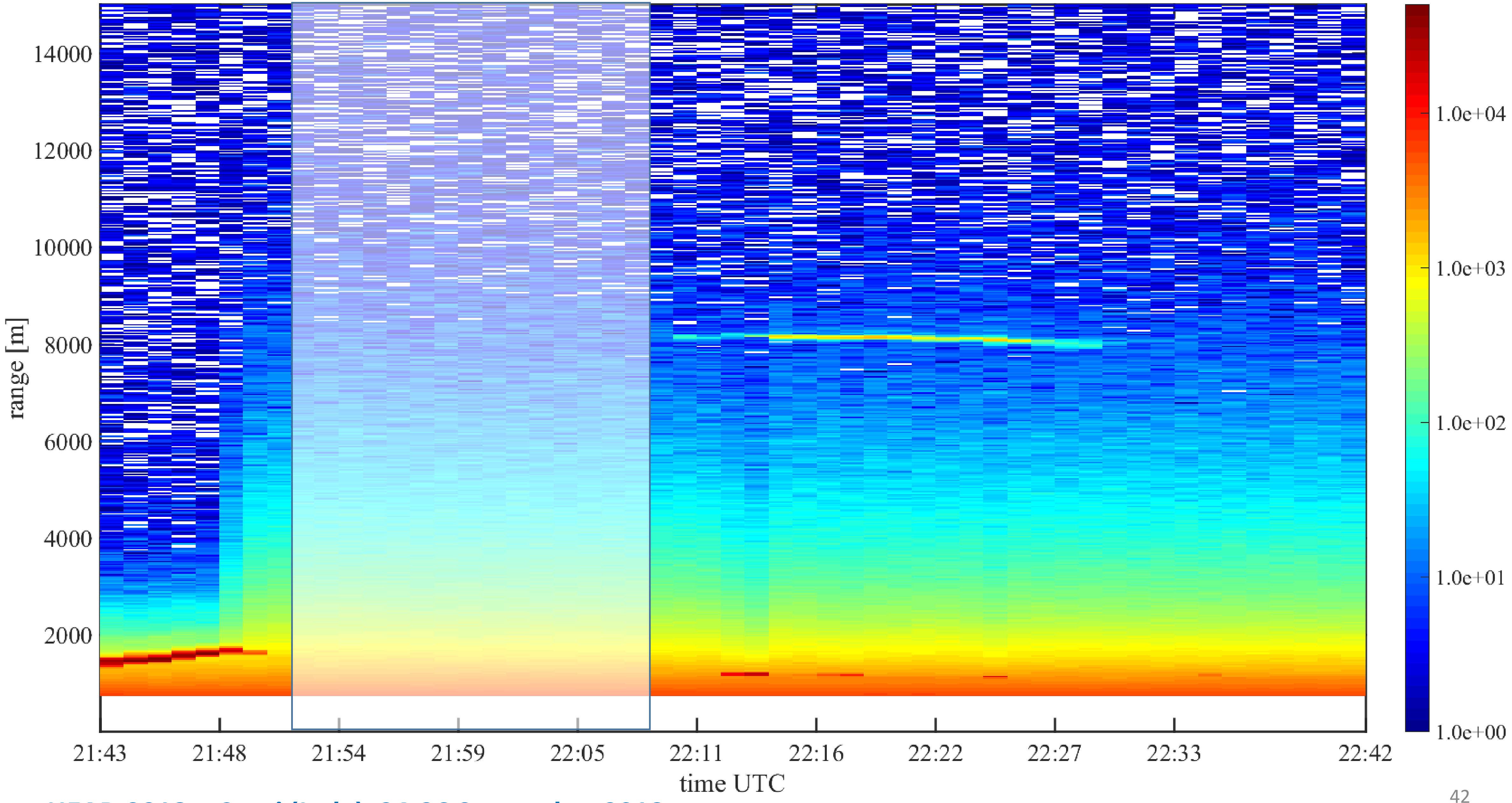

Derivative algorithm has a low pass digital filter embedded: **vertical resolution reduction because the removal of high frequency (small detail -> higher resolution).**

Finite impulse response (FIR) filter have:

$$y(n) = \sum_{k=-N}^{N} h(k)x(n-k)$$

The above Eq. is a representation of the *non-causal* **Linear Time Invariant (LTI) Finite Impulse Response (FIR) digital filter**, whose **frequency response** is:

$$H(\omega) = \sum_{k=-N}^{N} h(k)e^{-j\omega k}$$

•Aerosol & Water Vapor profiles

NOISE REDUCTION RATIO:

$$\mathrm{NRR} = \frac{\mathrm{Var}_{\mathrm{OUT}}}{\mathrm{Var}_{\mathrm{IN}}} = \sum_{k=-N}^{N} [h(k)]^2$$

The ERes can be written by means of a general equation that depends only to the low-pass filter chosen:

$$\Delta R_{\mathrm{eff}}^{\mathrm{L}(\hat{p})}|_{\mathrm{NRR}} = \frac{\Delta R_{\mathrm{raw}}}{\mathrm{NRR}^{\mathrm{L}(\hat{p})}}$$

•Aerosol & Water Vapor profiles

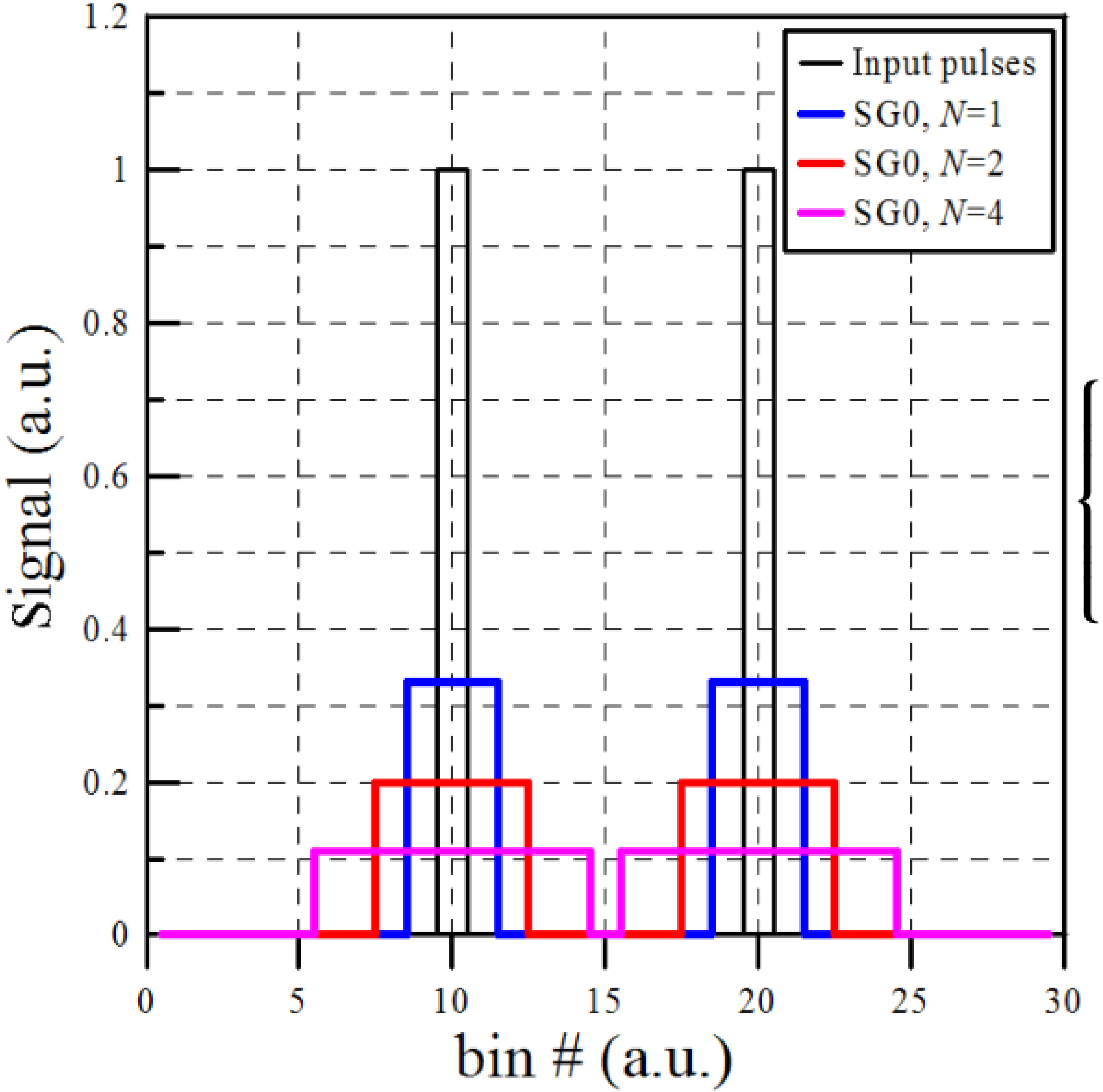

$$\mathrm{NRR} = \frac{\mathrm{Var}_{\mathrm{OUT}}}{\mathrm{Var}_{\mathrm{IN}}} = \sum_{k=-N}^{N} [h(k)]^2$$

$$\begin{cases} \mathrm{NRR}^{\mathrm{SG0(N)}} = \sum_{k=-N}^{N} [h^{\mathrm{SG0}}(k)]^2 = \dfrac{1}{2N+1}; \\ \Delta R_{\mathrm{eff}}^{\mathrm{SG0(N)}}|_{\mathrm{NRR}} = (2N+1)\Delta R_{\mathrm{raw}} = \dfrac{\Delta R_{\mathrm{raw}}}{\mathrm{NRR}^{\mathrm{SG0(N)}}}. \end{cases}$$

$$\Delta R_{\mathrm{eff}}^{\mathrm{L}(\hat{p})}|_{\mathrm{NRR}} = \frac{\Delta R_{\mathrm{raw}}}{\mathrm{NRR}^{\mathrm{L}(\hat{p})}}$$

Smoothing Optimization

The smoothing of a signal could not always lead to significant improvement in the SNR (saturation effect when almost all the noise is removed).
For this reason, in a smoothing operation it seems very relevant to find the limit over which the (undesirable) distortion of an underlying input signal could become more relevant than the concurrent (desirable) decrease of the noise level.

•Aerosol & Water Vapor profiles

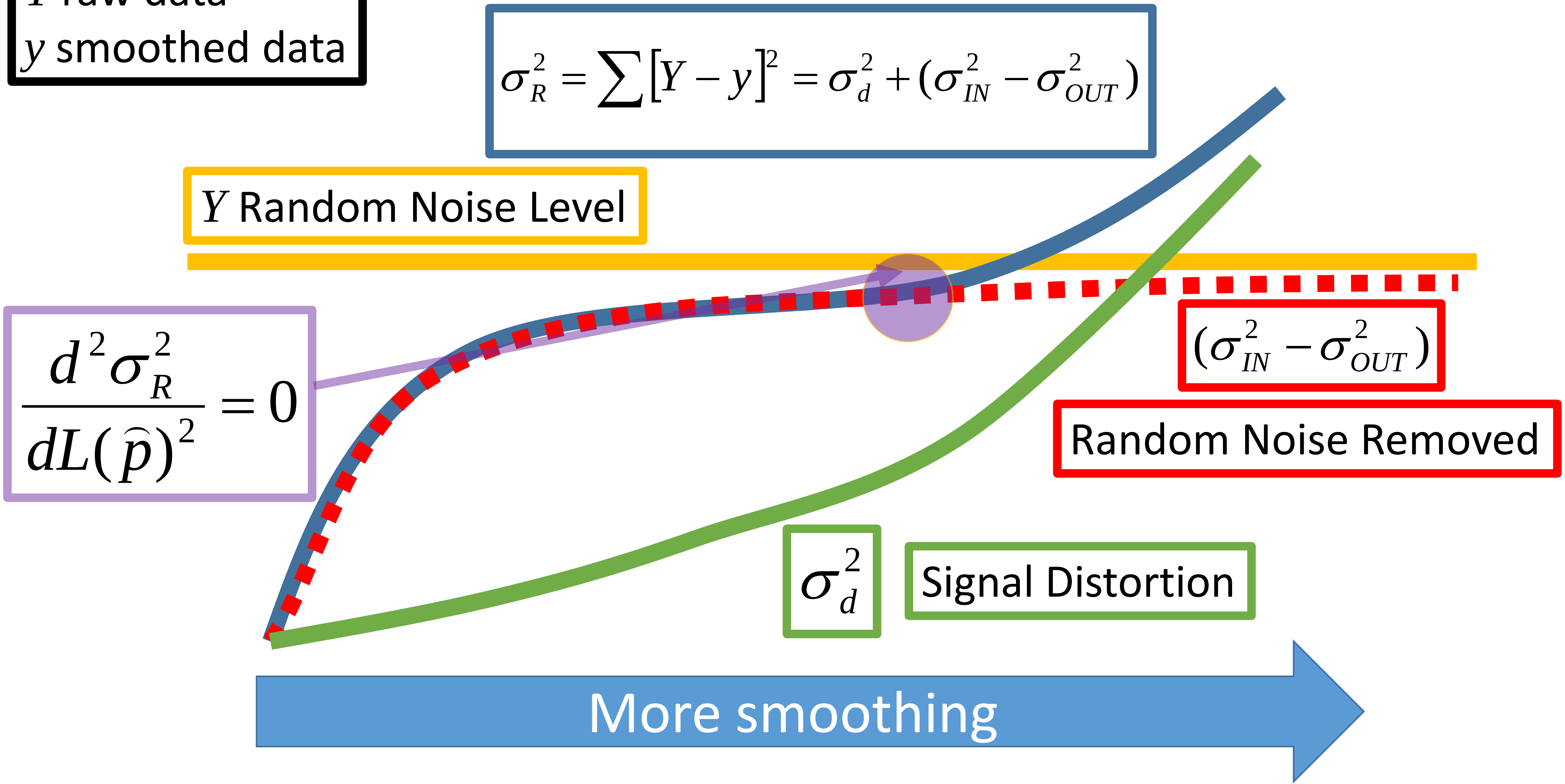

Y raw data

y smoothed data

$$\sigma_R^2 = \sum [Y - y]^2 = \sigma_d^2 + (\sigma_{IN}^2 - \sigma_{OUT}^2)$$

Y Random Noise Level

$$\frac{d^2 \sigma_R^2}{dL(\widehat{p})^2} = 0$$

$$(\sigma_{IN}^2 - \sigma_{OUT}^2)$$

Random Noise Removed

$$\sigma_d^2$$

Signal Distortion

More smoothing

•Aerosol & Water Vapor profiles

$$H^{(1)}(\omega) = j\omega = \omega e^{j\pi/2}, 0 \le \omega \le \pi;$$
$$|H^{(1)}(\omega)| = \omega.$$

…the goal is to design a band-limited differentiator that, for frequencies higher than a certain cut-off value, will ideally remove the high-frequency component:

$$H^{(1)\mathrm{L}}(\omega) = H^{(1)}(\omega) H^{\mathrm{L}}(\omega).$$

$$\boxed{H^{(1)\mathrm{L}}(\omega) = -j \sum_{k=-N}^{N} h^{(1)\mathrm{L}}(k) \sin(\omega k)}$$

$$\boxed{H^{\mathrm{L}}(\omega) = \frac{H^{(1)\mathrm{L}}(\omega)}{j\omega} = \frac{-\sum_{k=-N}^{N} h^{(1)\mathrm{L}}(k) \sin(\omega k)}{\omega}}$$

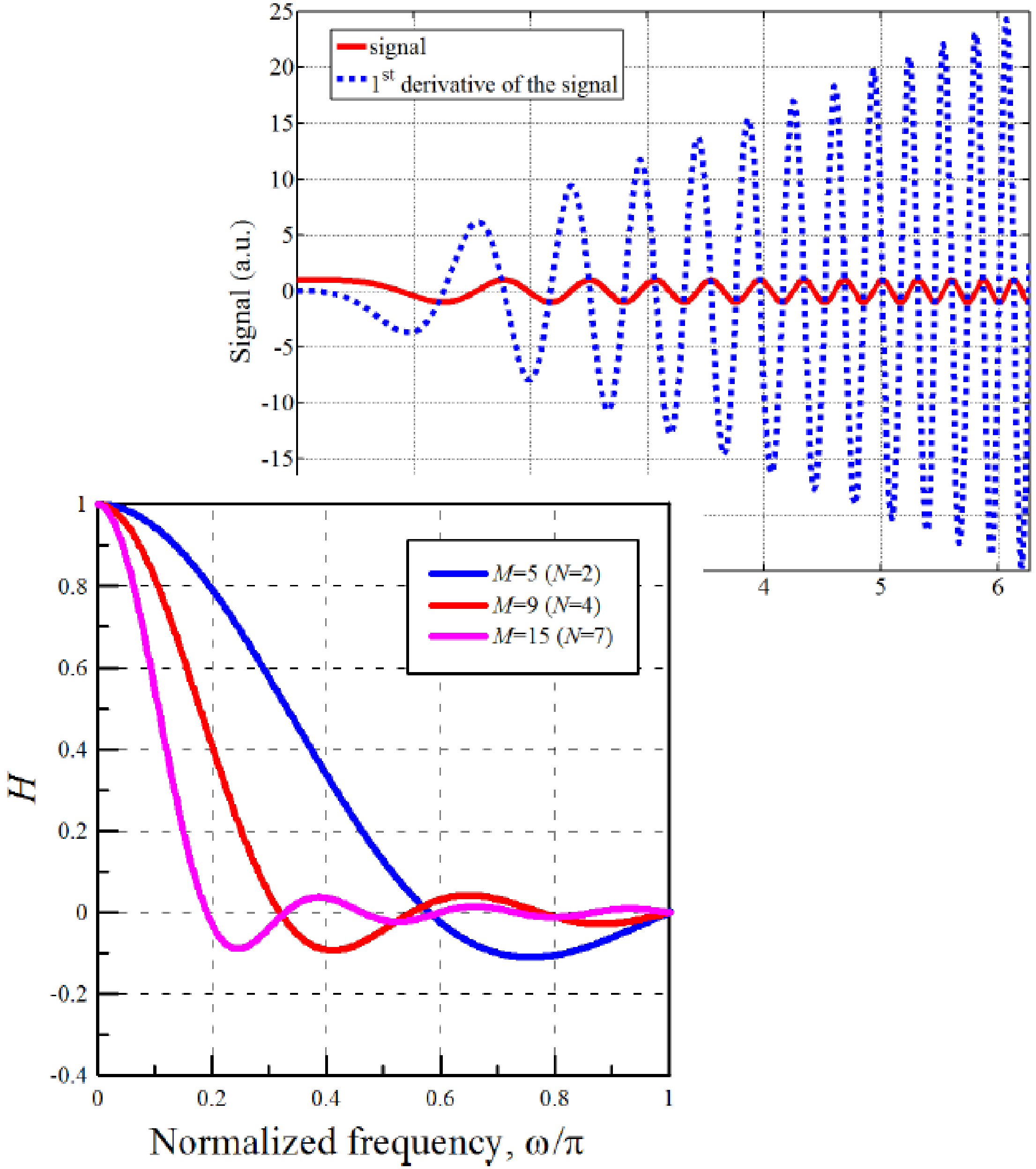

•Aerosol & Water Vapor profiles

“**Epic failures: 11 infamous software bugs**” reports as the most likely reason of **the Mariner 1 space mission failure was caused by a not smoothed time derivative** of a radius:

“…Without the smoothing function, even minor variations of the speed would trigger the corrective boosters to kick in. The automobile driving equivalent would be to yank the steering wheel in the opposite direction of every obstacle in the driver's field of vision…”.

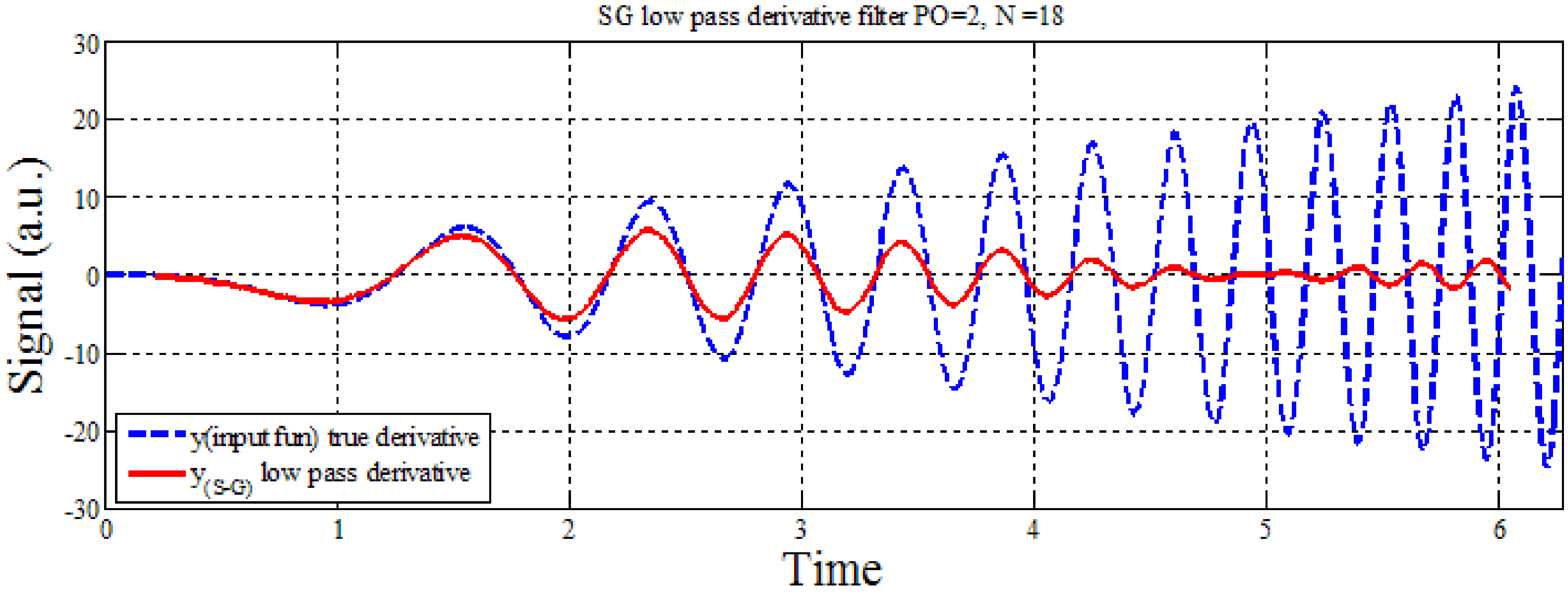

15 june 2018

Effective resolution from 300m to 1200m

- **Aerosol & Water Vapor profiles**

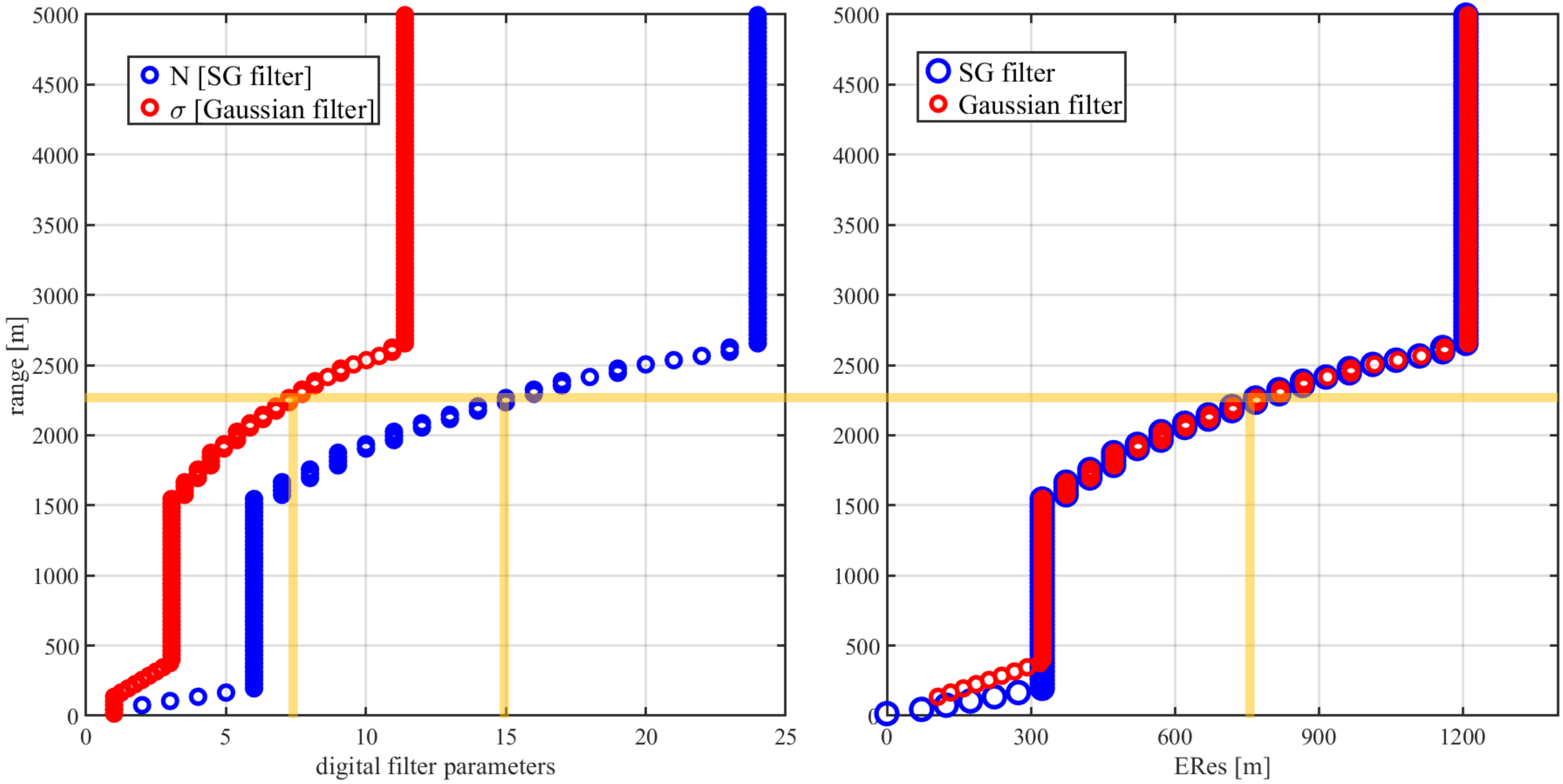

15 june 2018

•Aerosol & Water Vapor profiles

Same Effective resolution (750m)

-3dB level

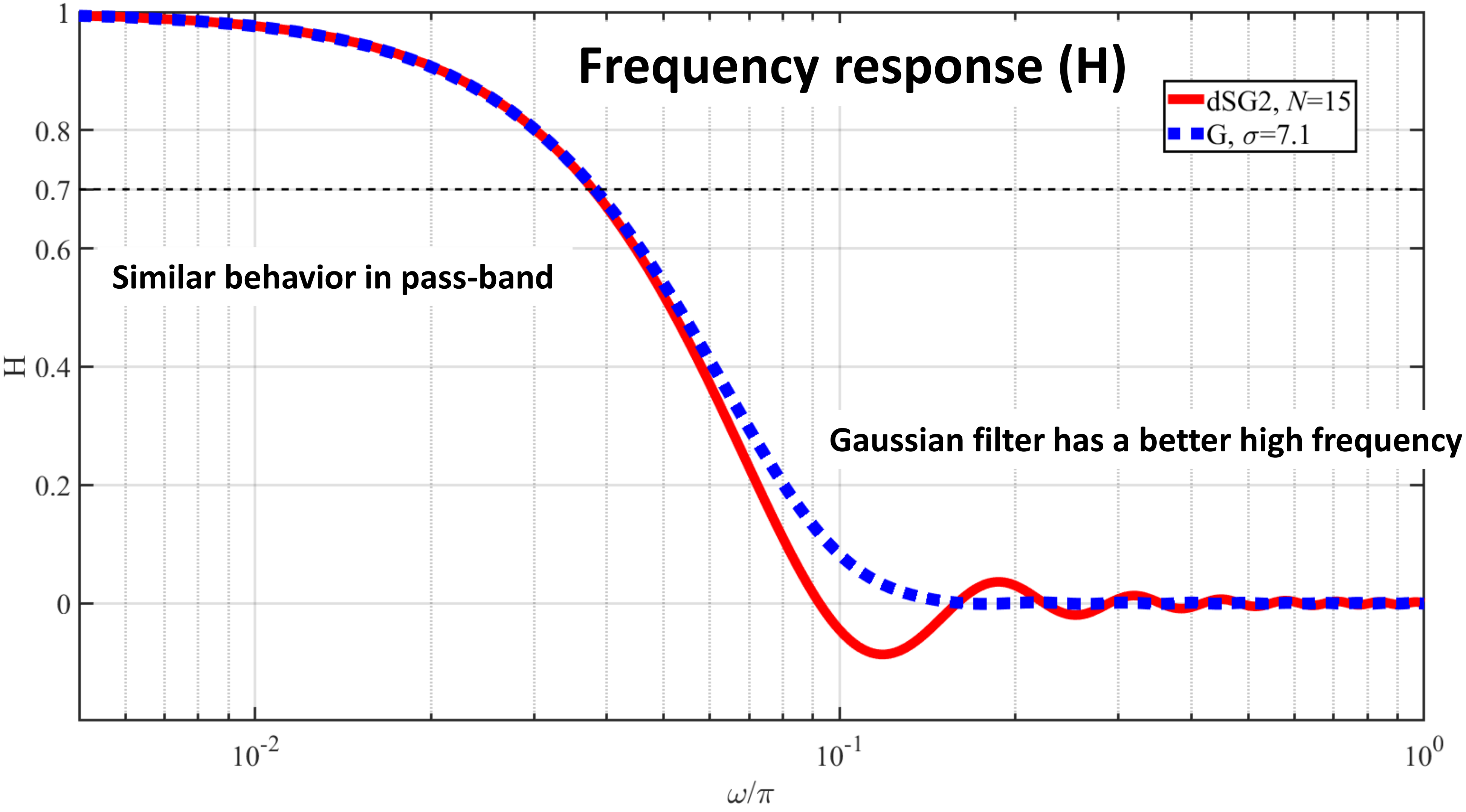

Similar behavior in pass-band

Gaussian filter has a better high frequency suppression

15 june 2018

- **Aerosol & Water Vapor profiles**

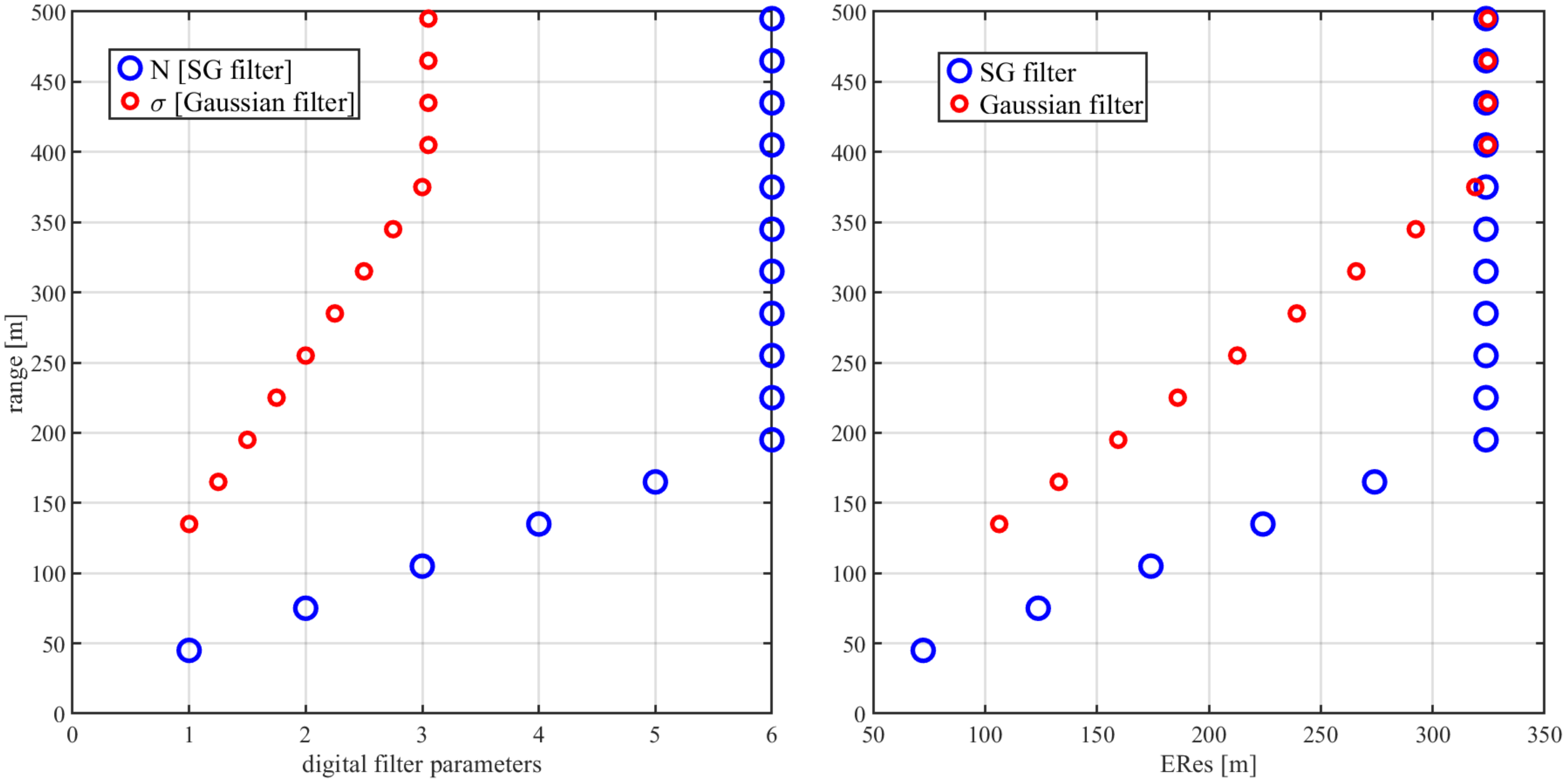

15 june 2018

•Aerosol & Water Vapor profiles

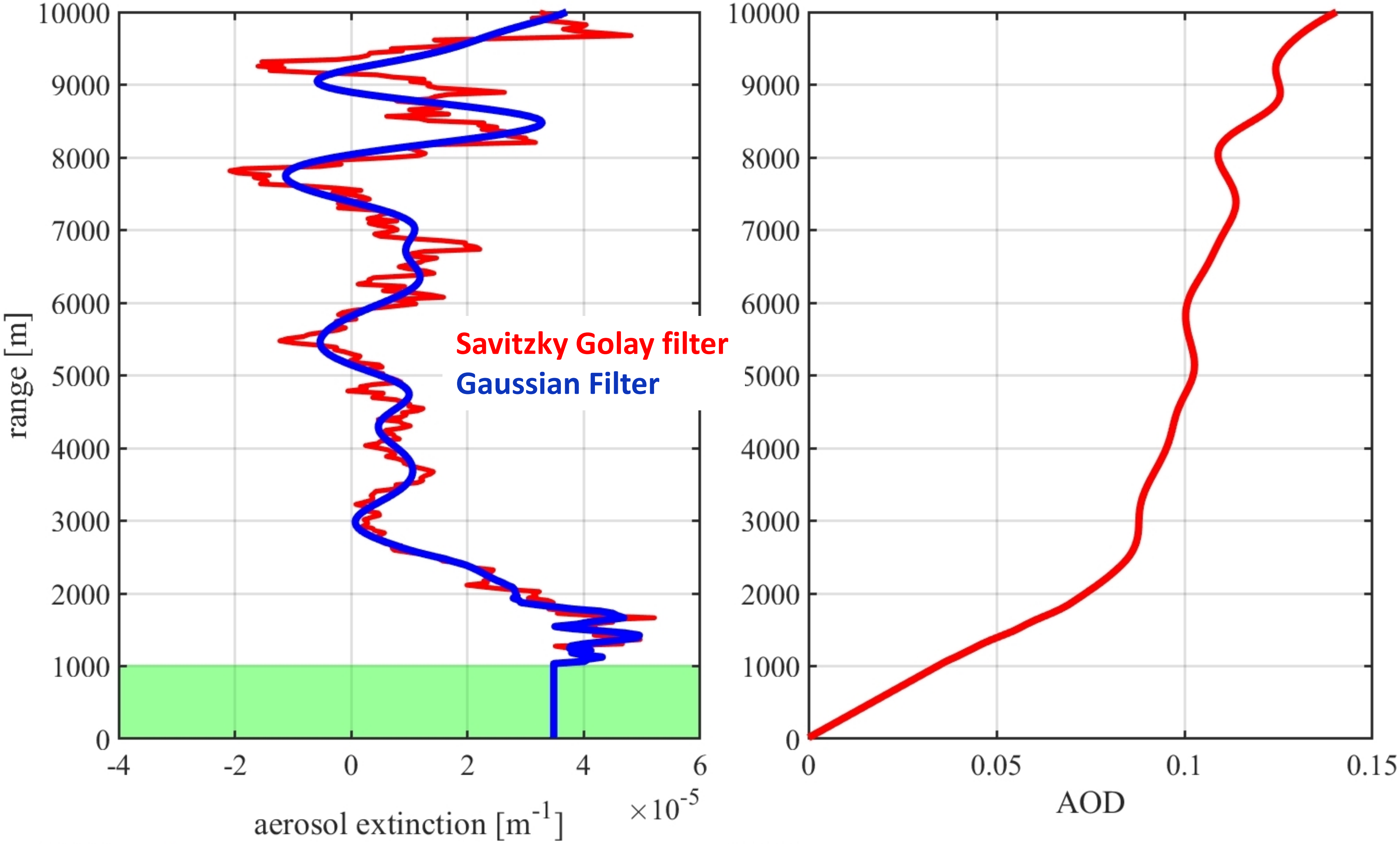

AtmoHEAD 2018 – Capri (Italy), 24-26 September 2018

15 june 2018

•Aerosol & Water Vapor profiles

AOD AERONET DATA

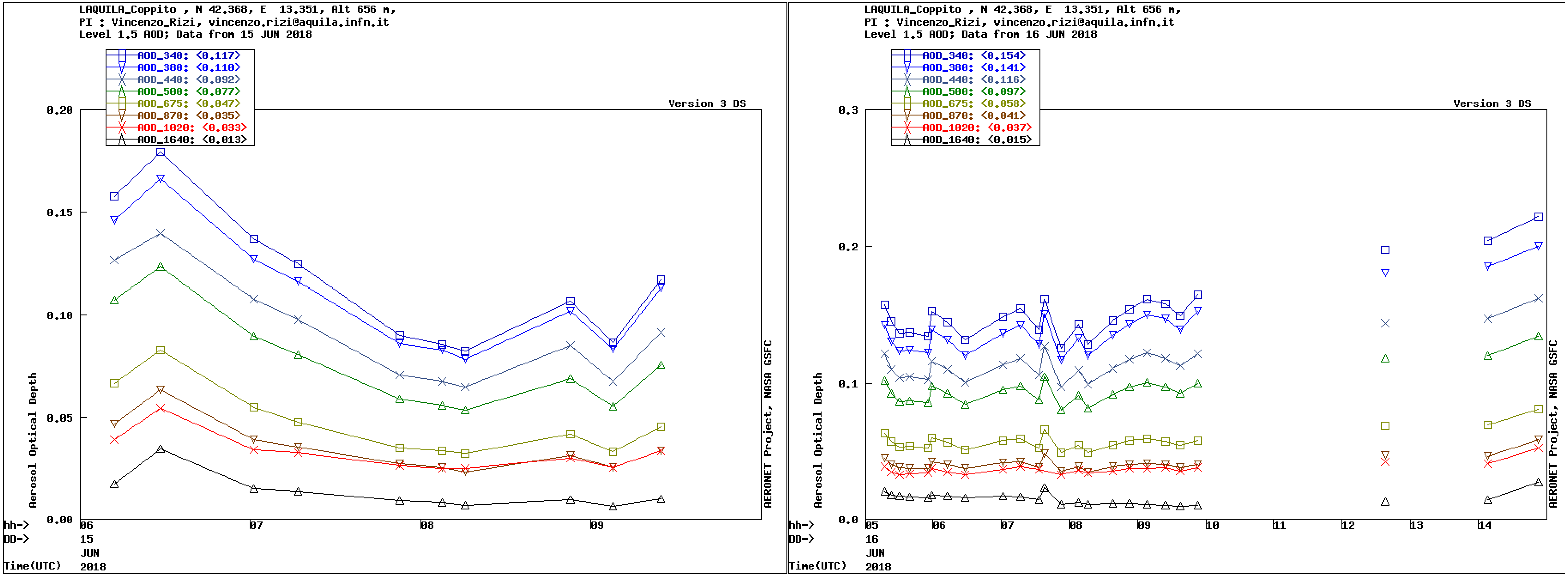

15 june 2018

•Aerosol & Water Vapor profiles

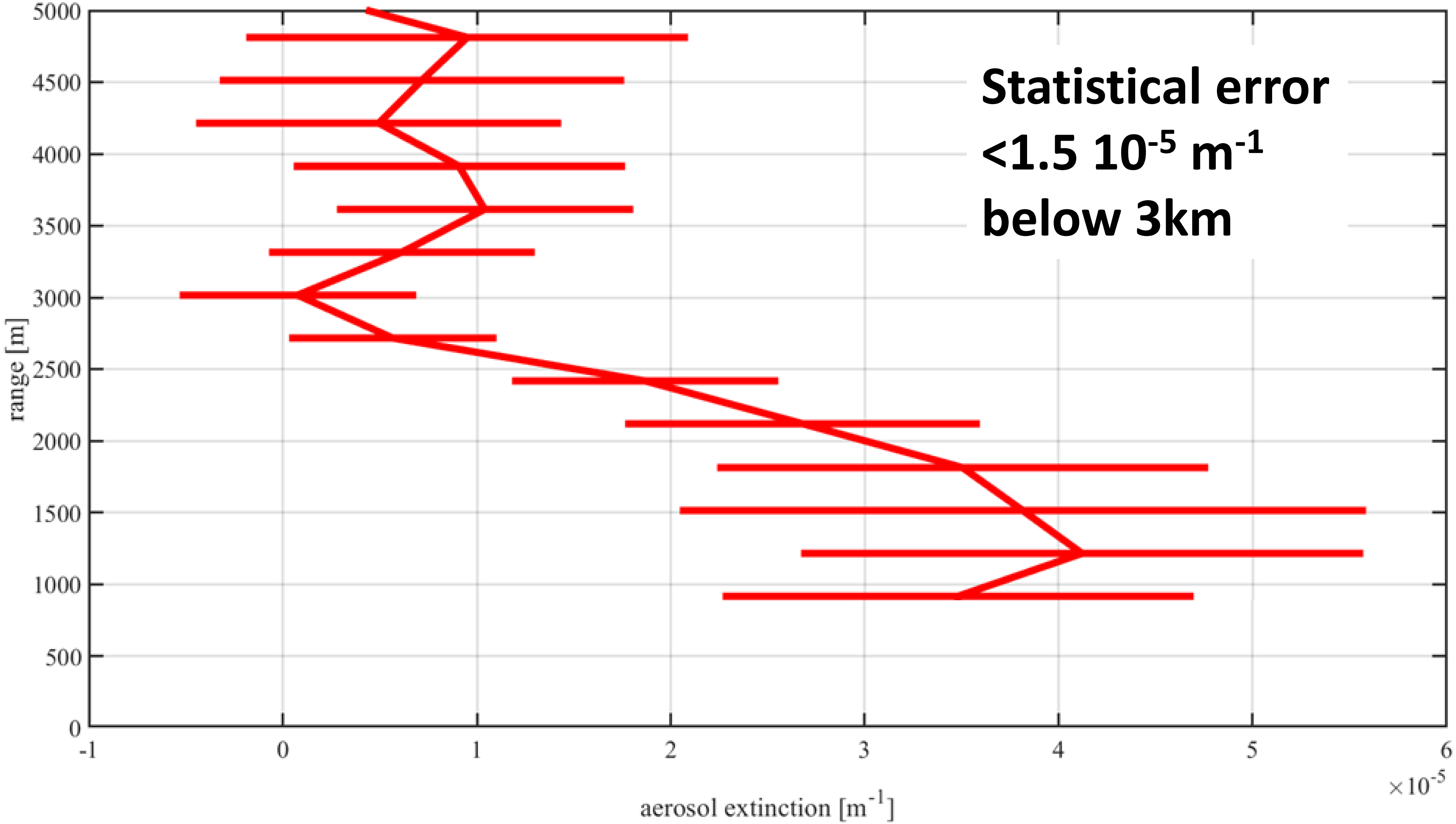

Statistical error
<1.5 10^{-5} m^{-1}
below 3km

•Aerosol & Water Vapor profiles

$$\tau_{aer}(z) = -\frac{log\left(\frac{K_{\lambda_R} z^2 P_{\lambda_R}(z)}{T_{mol,\lambda_0}(z)\,T_{mol,\lambda_R}(z)\,N_R(z)}\right)}{1+\left(\frac{\lambda_o}{\lambda_R}\right)^k}$$

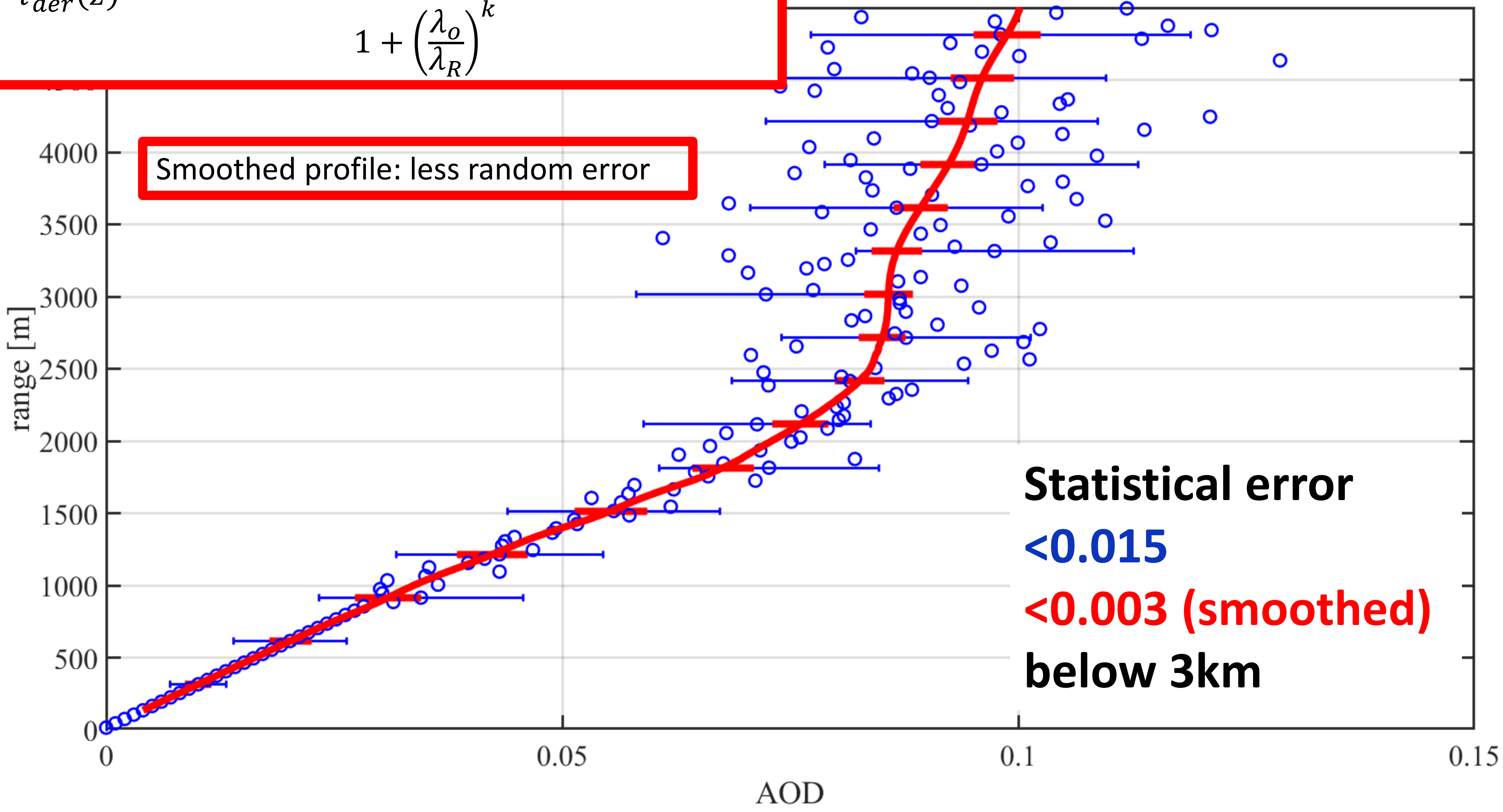

Smoothed profile: less random error

Statistical error

<0.015

<0.003 (smoothed)

below 3km

15 june 2018

•Aerosol & Water Vapor profiles

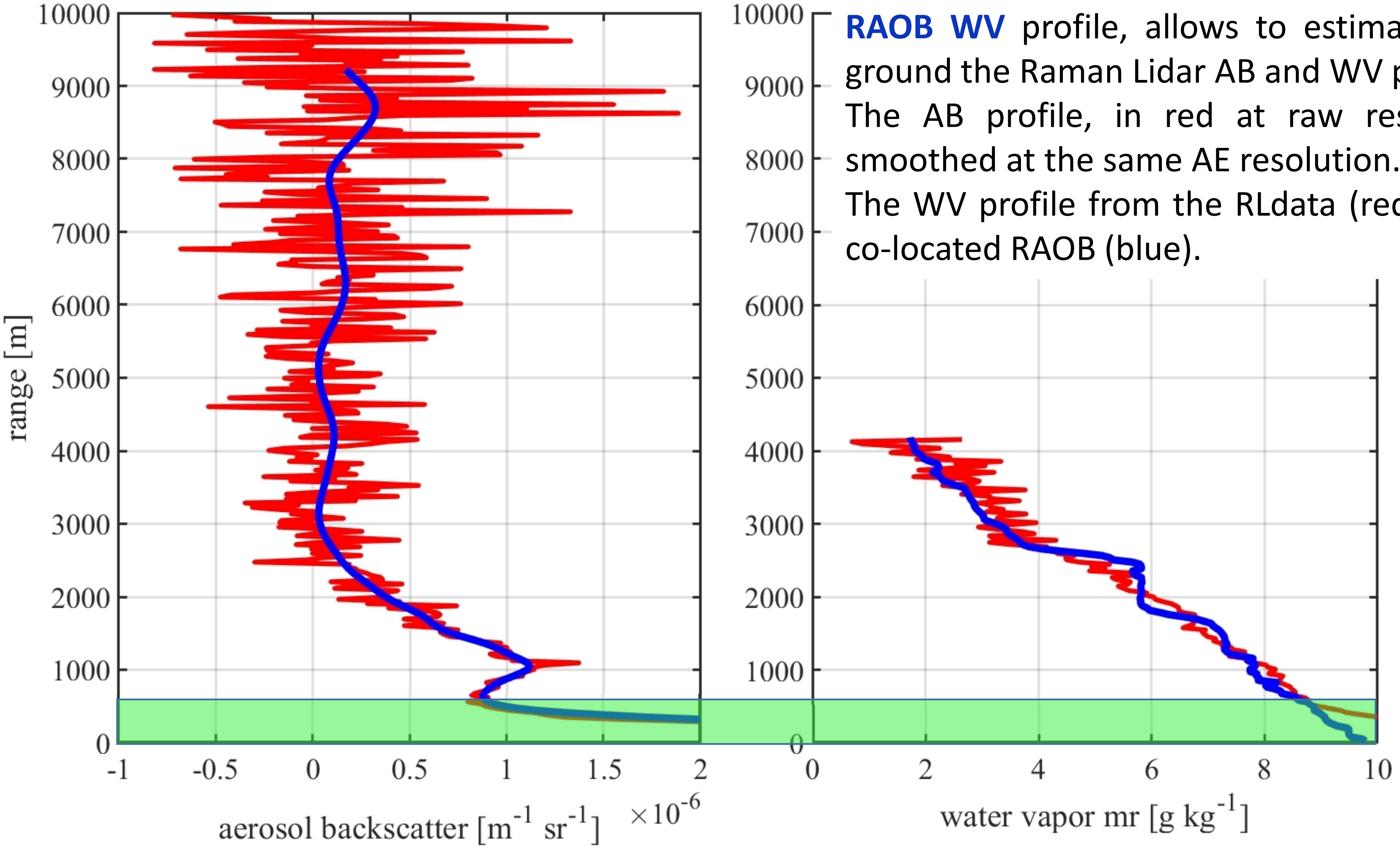

RAOB WV profile, allows to estimate how down to ground the Raman Lidar AB and WV profiles can go.

The AB profile, in red at raw resolution, in blue smoothed at the same AE resolution.

The WV profile from the RLdata (red) compared with co-located RAOB (blue).

•Aerosol & Water Vapor profiles

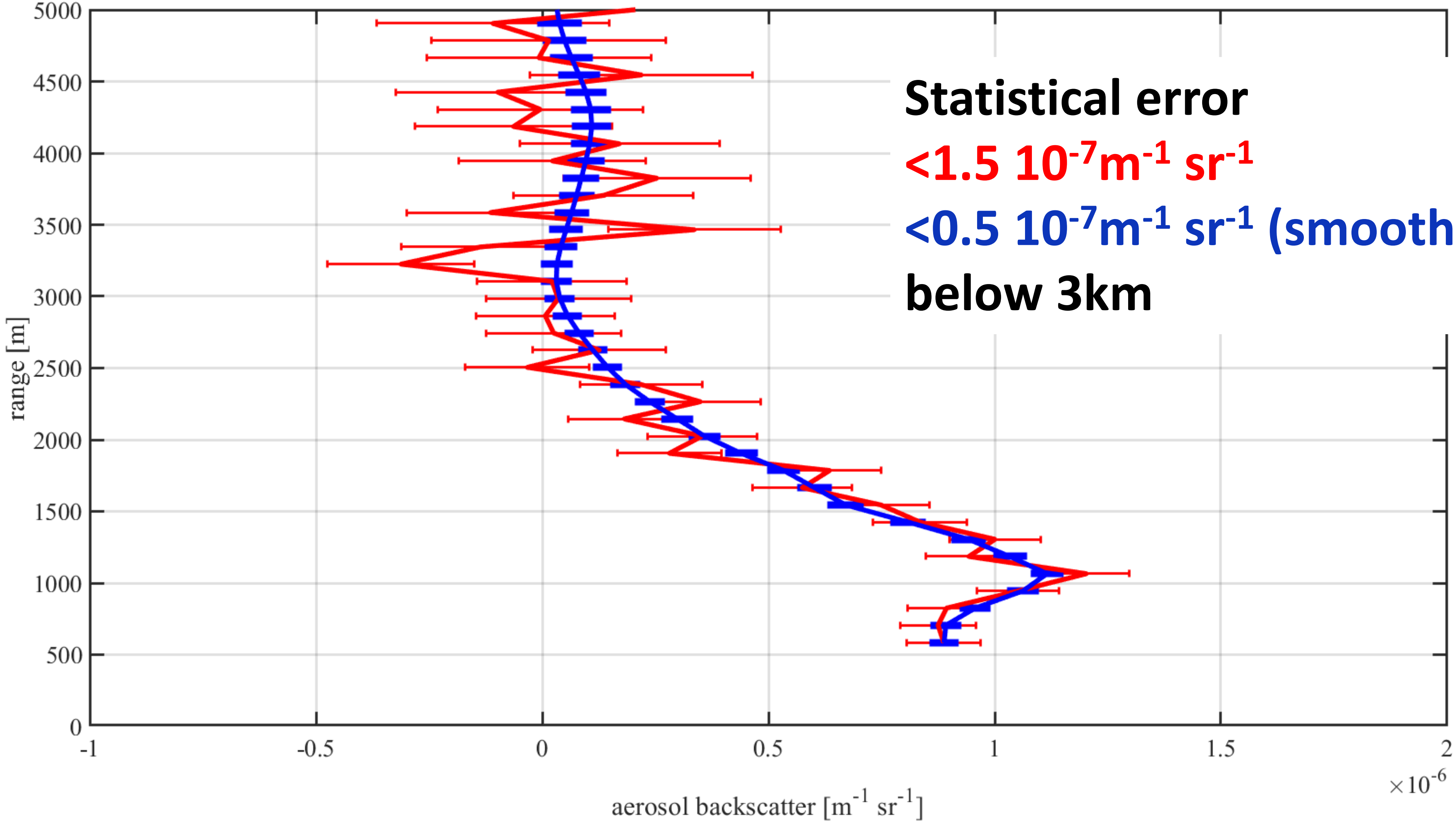

Statistical error

<1.5 $10^{-7} m^{-1} sr^{-1}$

<0.5 $10^{-7} m^{-1} sr^{-1}$ (smoothed)

below 3km

•Aerosol & Water Vapor profiles

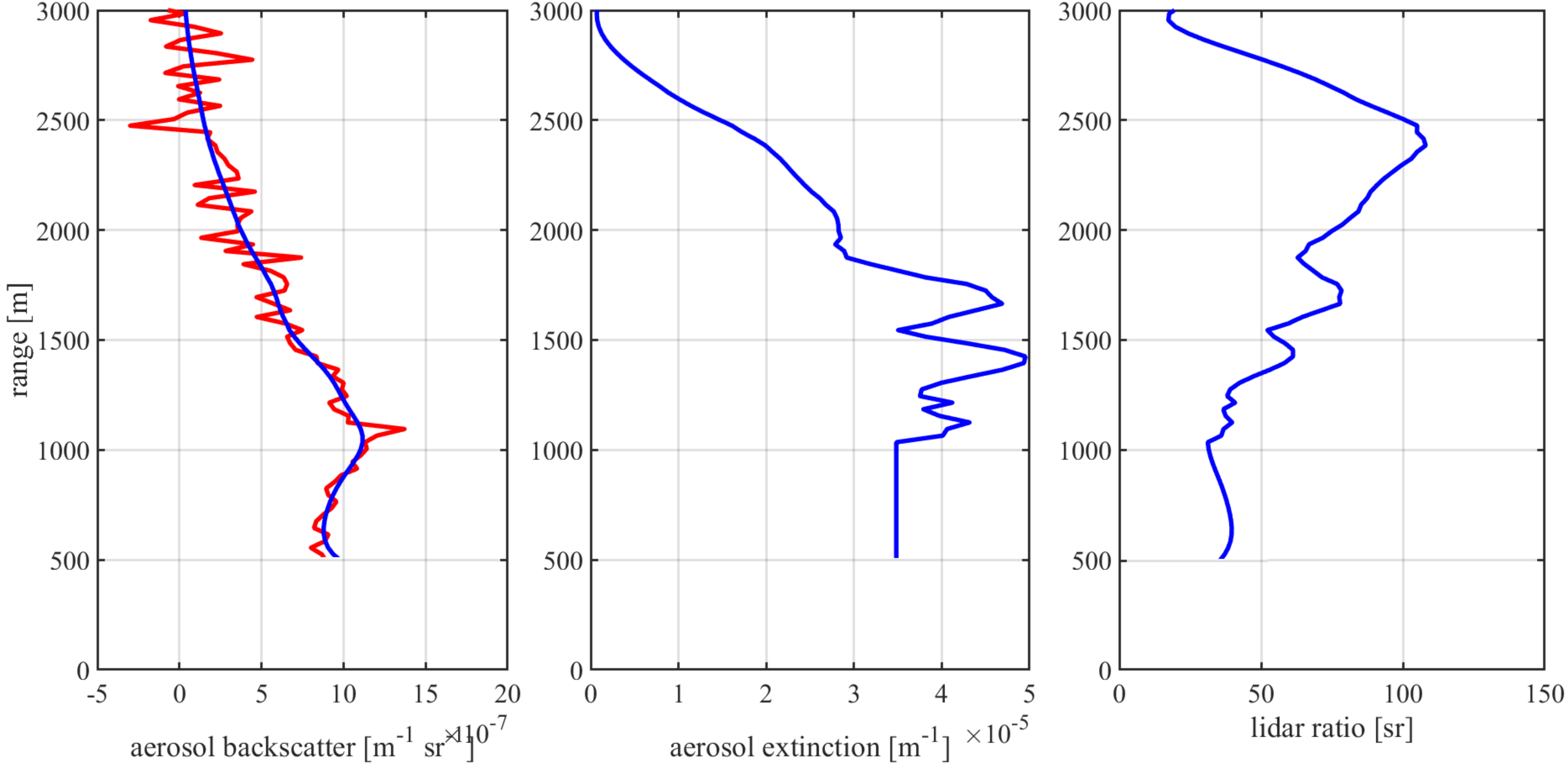

•Aerosol & Water Vapor profiles

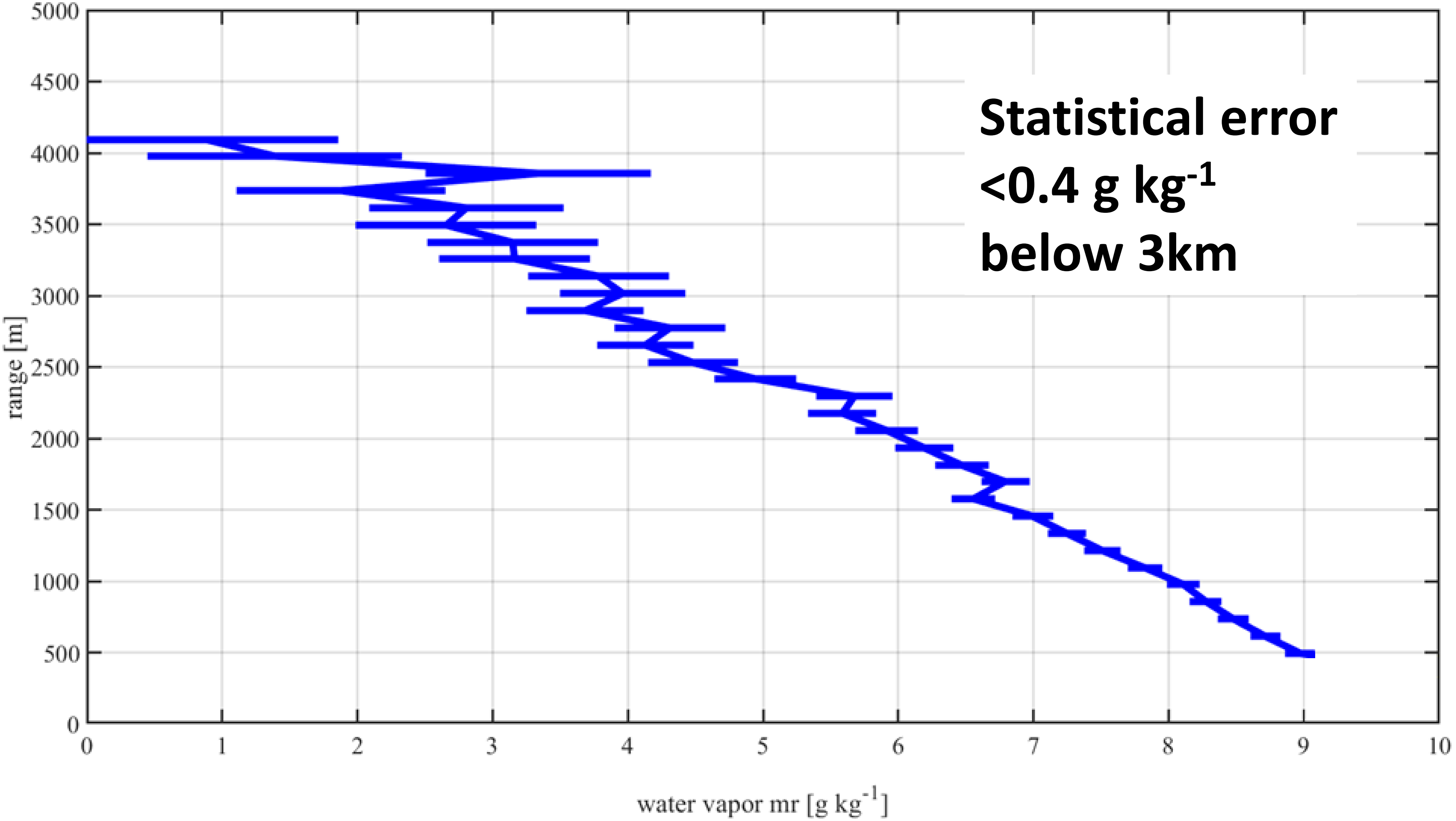

Statistical error
<0.4 g kg^{-1}
below 3km

From L'Aquila…

…To Turin…

… @ ORM

cta
cherenkov telescope array

ARCADE Raman lidar

INFN
Istituto Nazionale di Fisica Nucleare

Sezione di Torino
Sezione di Napoli
Gruppo Collegato GSSI L'Aquila

CETEMPS
DSFC

Università degli Studi dell'Aquila
Dipartimento di Scienze fisiche e chimiche
CETEMPS

Università degli Studi di Napoli Federico II
Dipartimento di Fisica «Ettore Pancini»

Conclusion

The ARCADE RL has been partially upgraded and extensively tested in L'Aquila:

- **The overall optical performances have been significantly improved.**
- **A number of practical standard procedure have been developed to setup the system for automatic measurements once in ORM.**
- **An efficient DAQ control software and a certified lidar signals inversion code have been also developed in house.**
- **Further optimization of the system in both the hardware and software section are possible in order to reduce the uncertainties.**
- **We expect that the system will be operative from the second week of October 2018.**

EXPERIMENTAL SETUP

MEASUREMENTS WITH FAST-PHOTODIODE

trigger configuration of DAQs

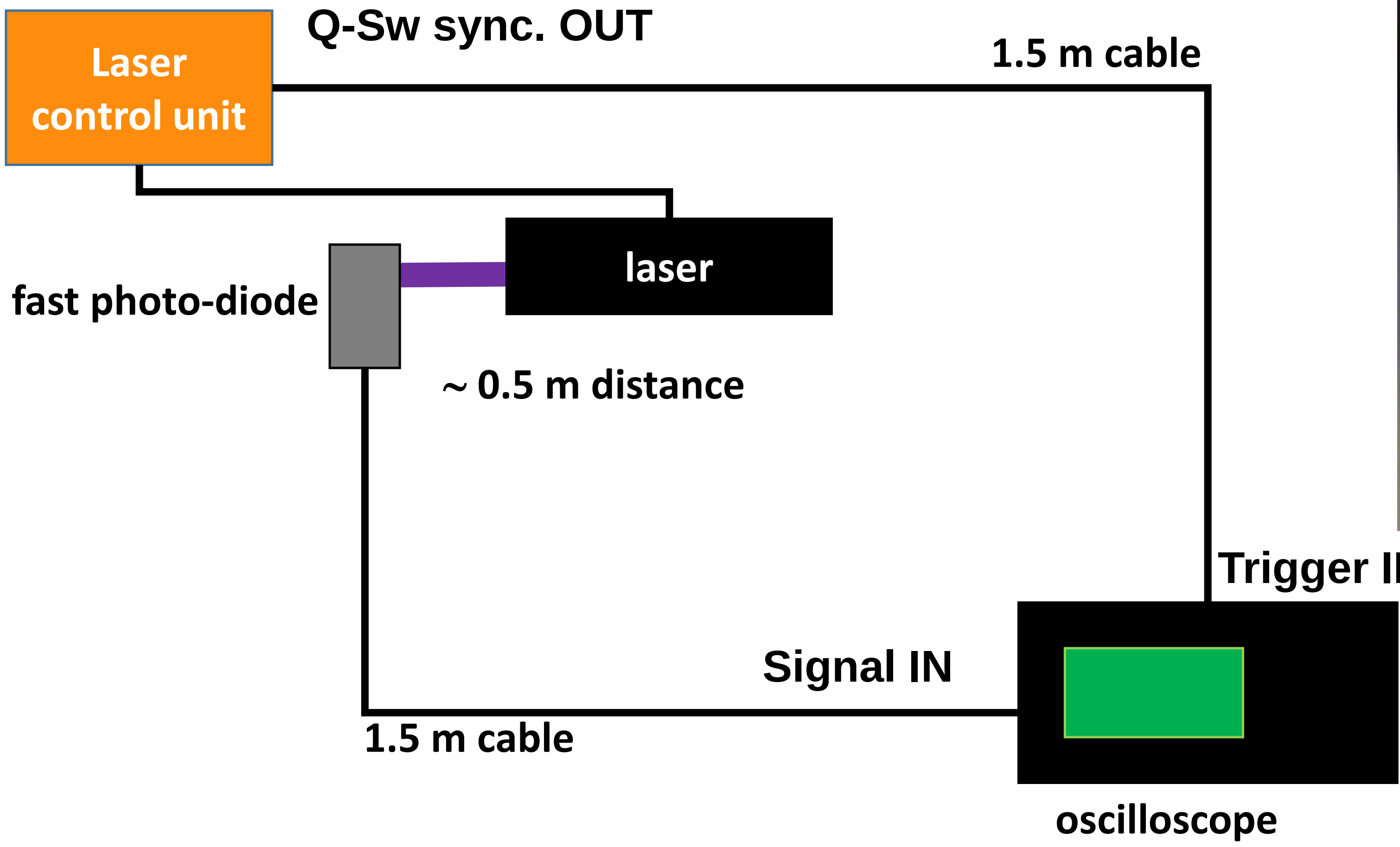

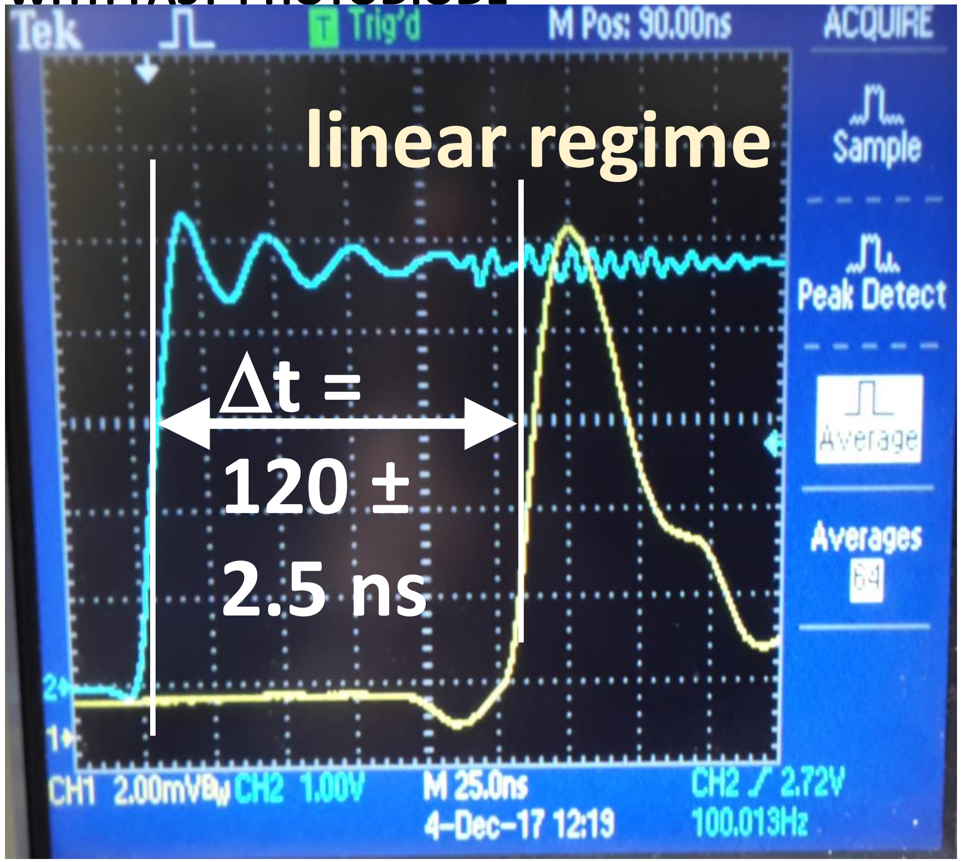

The trigger-laser light out delay ($\Delta\tau_L$) is:
$\Delta\tau_L$ = Δt [120.0 ± 2.5 ns] +
– [photodiode trans. time ([2-3 ns ± 2 ns) +
[+ 1.5 m BNC (7.5 ± 1 ns) - 1.5 m BNC (7.5 ± 1 ns)]- [laser path in air (2 ns)]= 115ns ± 5ns

•Aerosol & Water Vapor profiles

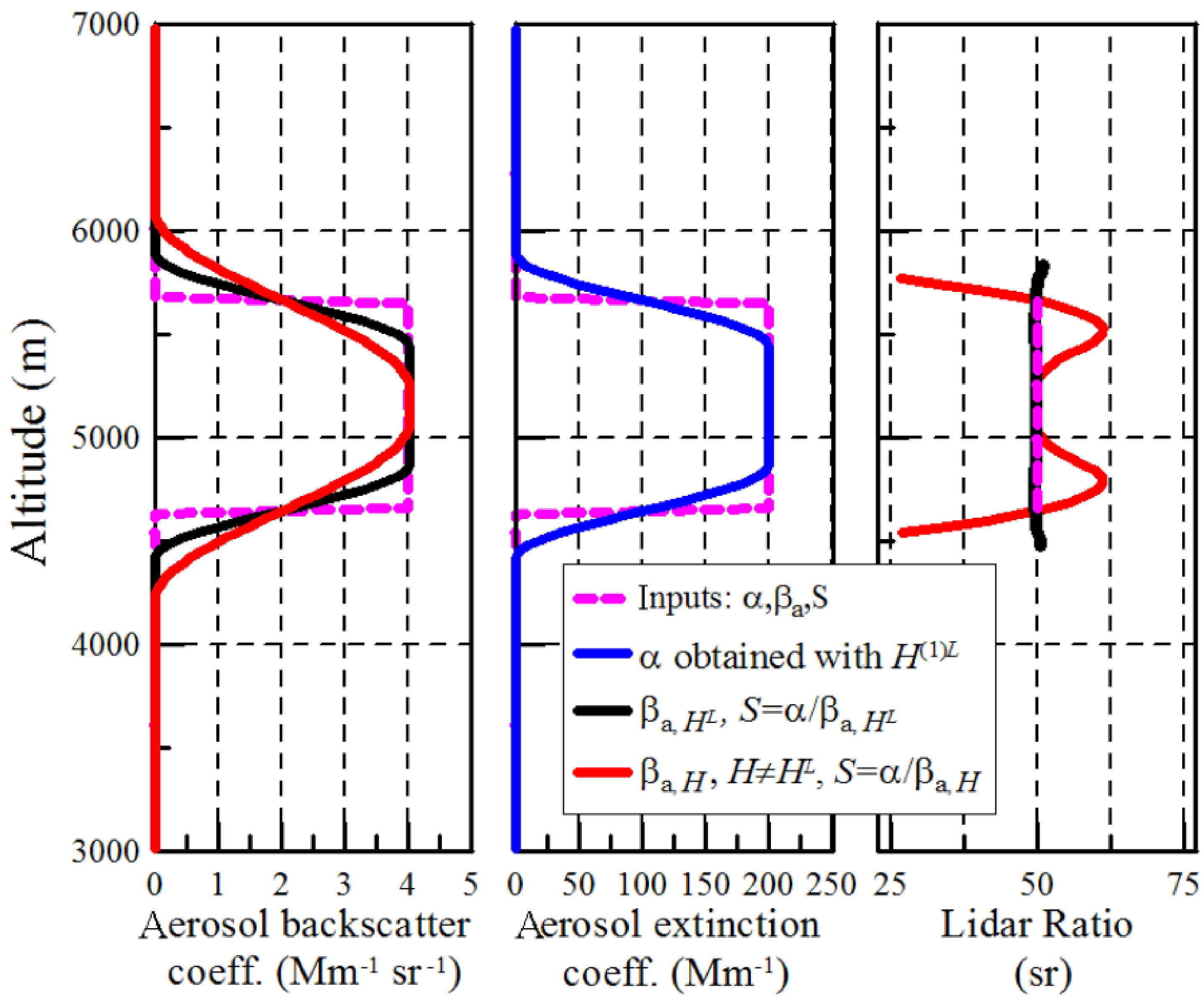

Rayleigh Fit

•Aerosol & Water Vapor profiles